

Growth and Characteristics of Bulk Single Crystals Grown from Solution on Earth and in Microgravity

M. D. Aggarwal⁺, A. K. Batra, R. B. Lal

**Department of Physics, P.O. Box 1268
Alabama A&M University
Normal, AL 35762, USA**

Benjamin G. Penn and Donald O. Frazier

NASA / Marshall Space Flight Center, Huntsville, AL 35812, USA

ABSTRACT

The growth of crystals has been of interest to physicists and engineers for a long time because of their unique properties. Single crystals are utilized in such diverse applications as pharmaceuticals, computers, infrared detectors, frequency measurements, piezoelectric devices, a variety of high technology devices and sensors. Solution crystal growth is one of the important techniques to grow a variety of crystals when the material decomposes at the melting point and a suitable solvent is available to make a saturated solution at a desired temperature. In this chapter an attempt is made to give some fundamentals of growing crystals from solution including improved designs of various crystallizers. Since the same solution crystal growth technique could not be used in microgravity, authors had proposed a new cooled sting technique to grow crystals in space. Authors' experiences of conducting two space shuttle experiments relating to solution crystal growth are also detailed in this work. The complexity of these solution growth experiments to grow crystals in space are discussed. These happen to be some of the early experiments performed in space, and various lessons learnt are described. A brief discussion of protein crystal growth that also shares basic principles of solution growth technique is given along with some flight hardware information for its growth in microgravity.

Key Words: Solution crystal growth; Microgravity; Triglycine sulfate; Protein crystals, Spacelab-3, International Microgravity Laboratory-1

⁺ Present Address: NASA Administrator's Fellow, EV-43 ISHM and Sensors Branch, NASA /Marshall Space Flight Center, Huntsville, AL 35812, USA

Contents

- 1.0 INTRODUCTION
- 2.0 CRYSTALLIZATION: NUCLEATION AND GROWTH KINETICS
 - 2.1 Expression for supersaturation
 - 2.2 Effects of convection in solution growth
 - 2.2.1 Natural convection
 - 2.2.2 Forced convection
 - 2.3 Effect of impurities
- 3.0 CLASSIFICATION OF CRYSTAL GROWTH
- 4.0 LOW TEMPERATURE SOLUTION GROWTH
 - 4.1 Solution growth methods
 - 4.1.1 Slow cooling method
 - 4.1.2 Slow evaporation method
 - 4.1.3 Temperature gradient method
 - 4.1.4 Chemical/Gel method
- 5.0 SOLUTION GROWTH BY TEMPERATURE LOWERING
 - 5.1 Solvent selection and solubility
 - 5.1.1 Solubility determination
 - 5.2 Design of a crystallizer
 - 5.2.1 A Typical solution crystal growth crystallizer
 - 5.2.2 Crystal seed-holder
 - 5.2.3 Preparation of seed crystal and mounting
 - 5.3 Solution preparation and starting a growth run
- 6.0 TRIGLYCINE SULFATE CRYSTAL GROWTH– A CASE STUDY
 - 6.1 Growth of single crystals of triglycine sulfate
 - 6.2. Growth kinetics and habit modification
 - 6.2.1 Effect of seed crystal
 - 6.2.2 Effect of growth temperature and supersaturation
 - 6.2.3 Effect of pH of the solution
 - 6.2.4 Effect of impurities

7.0 SOLUTION GROWTH OF TRIGLYCINE SULFATE CRYSTALS IN
MICROGRAVITY ABOARD SPACELAB-3 AND IML-1

7.1 Rationale for solution crystal growth in space

7.2 Crystal growth method in space

7.2.1 Cooled sting technique

7.2.2 Flight hardware

7.2.3 Flight optical system

7.3 Results and Discussion

8.0 PROTEIN CRYSTAL GROWTH

8.1 Protein crystal growth methods

8.2 Protein crystal growth mechanisms

8.3 Protein crystal growth in microgravity

9.0 CONCLUDING REMARKS

Acknowledgements

References

1.0 INTRODUCTION

The growth of crystals with tailored physical and chemical properties, characterization of crystals with advanced instrumentation and their eventual conversion into devices, play a vital role in science and technology. Crystal growth is an important field of materials science, which involves controlled phase transformation. Growth of crystals from solution at low temperature is one of the important techniques in the field of science: pharmaceutical, agriculture and materials science. Crystal growth acts as a bridge between science and technology for practical applications. In the past few decades, there has been a growing interest in the crystal growth process, particularly in view of the increasing demand for materials for technological applications. The strong influence of single crystals in the present day technology is evident from the recent advancements in the fields of semiconductors, transducers, infrared detectors, ultrasonic amplifiers, ferrites, magnetic garnets, solid state lasers, nonlinear optic, piezoelectric, acousto-optic, photosensitive materials and crystalline thin films for microelectronics and computer applications. All these developments could be only achieved due to the availability of single crystals such as silicon, germanium, gallium arsenide, and also with the discovery of nonlinear optical properties in some inorganic, semi-organic and organic crystals. Researchers have always been in the search of new materials for the growth of single crystals for new applications and modifying present crystals for various applications. Any crystal growth process is complex; it depends on many parameters which can interact. A complete description of a process may well be impossible, since it would require the specifications of too many variables. That is why, sometimes crystal growth is called art and science but like other crafts, it can provide great satisfaction after a successful crystal growth of a desired material.

The solid-state materials can be classified into single crystals, polycrystalline, and amorphous materials depending upon the arrangement of constituent molecules, atoms or ions. An ideal crystal is one, in which the surroundings of any atom would be exactly the same as the surroundings of every similar atom in three dimensions. Real crystals are finite and contain defects. The consistency of the characteristics of devices fabricated from a crystal depends on the homogeneity and defect contents of the crystals. Hence, the process of producing single crystals, which offer homogeneous media in the

atomic level with directional properties, attracts more attention than any other process. The methods of growing crystals are mainly dictated by the characteristics of the material and the desired size of the crystal. The method of growing crystals at low and high temperature can be broadly divided into the following six categories: (i) Growth from aqueous solution (low temperature growth); (ii) Growth by gel method (low temperature growth); (iii) Growth from flux or top seeded solution growth method (high temperature growth); (iv) Hydrothermal growth (high temperature growth); (v) High pressure growth (high temperature growth); and (vi) Growth by electrodeposition

Growth of bulk crystals from aqueous solution is technically very important. Besides bulk crystal growth, this method is also used for the purification of materials and the separation of impurities. Growth of large single crystals from aqueous solution is of interest for essentially two reasons. First, there is a growing need for solution-grown crystals in the area of high-power laser technology like potassium dihydrogen phosphate (KDP) type crystals. Second, research on this area of crystal growth and the corresponding in-depth examination of several key parameters provides fundamental case studies generating theory and technology, applicable to all of solution crystal growth processes, including new aqueous growth systems and high temperature solution growth.

In this chapter, the fundamental aspects of solution growth and the different methods of bulk crystal growth from solution are described along with solution crystal growth in the microgravity environment of space. Based on extensive experience of the authors in growing inorganic and organic crystals on earth and in space, the authors have tried to give a lucid explanation of the fundamentals of solution crystal growth and crystal growth systems. However, enough details are given on fabrication of crystallizers, associated instruments, and techniques so that new researcher may be able to design and set up his/her own solution crystal growth system after review of this chapter. Furthermore, growth and perfection of technologically important crystal from aqueous solution based on a case study of triglycine sulfate is presented. Effects of various parameters such as design of the seed holder, seed morphology, characteristics of the solution such as pH, temperature of growth, dopants, impurities; and microgravity on the physical properties are presented in detail.

2.0 CRYSTALLIZATION: NUCLEATION AND GROWTH KINETICS

The study and investigation of crystal growth implies the determination of growth laws, growth mechanisms and explanation of final result, i.e. the crystal habit. These aspects are interconnected. Since the growth rate of a face depends on its growth mechanisms and contributes to define the crystal habit, the detailed knowledge of these aspects is essential for the production of crystals of specific physical or morphological properties. The crystal growth is due to deposition of solute particles on the crystal faces, which can grow layer by layer at different rates. The growth rate of a face, i.e. advancement of its surface in the normal direction per unit time, depends upon internal and external factors. Internal factors are the surface structure of faces, which in turn are related to the bulk crystal structure, and their degree of perfection. Defects usually occur in the crystals and can emerge at the surface, affecting the growth kinetics. External factors are supersaturation, solute concentration which is related to solubility, temperature of the solution, solution composition, mechanical conditions such as still or stirred solution, presence of impurities, magnetic field, and gravitational field. The crystal growth of a face is a succession of complex processes, which take place at the interface between the liquid and solid phase. It therefore implies transport of matter and energy across the interface, which is the site of major importance in crystal growth.

In the following section, the fundamentals of nucleation and crystal growth at low temperature solution are described.

2.1 Expression for supersaturation

The supersaturation of a system can be expressed in a number of ways. A basic unit of concentration as well as temperature must be specified. The concentration driving force (ΔC), the supersaturation ratio (S) and relative supersaturation (σ) are related to each other as follows:

The concentration driving force

$$\Delta C = C - C^* \quad (1)$$

where C is the actual concentration of the solution and C^* is the equilibrium concentration at a given temperature.

Supersaturation ratio

$$S = C/C^* \quad (2)$$

Relative supersaturation,

$$\sigma = (C - C^*)/C^* \quad \text{or} \quad \sigma = S - 1 \quad (3)$$

If the concentration of a solution can be measured at a given temperature and the corresponding equilibrium saturation concentration is known, then the supersaturation can be estimated.

The required supersaturation can be achieved either by cooling/evaporation or addition of a precipitant. Meirs and Isaac reported a detailed investigation on the relationship between supersaturation and spontaneous crystallization [1]. The results of their analysis are shown in Fig. 1. It shows three zones, which are termed as region I, II and III. The lower continuous line is the normal solubility of the salt concerned. Temperature and concentration, at which spontaneous crystallization occurs, are represented by the upper broken curve, generally referred as the super-solubility curve. This curve is not well defined as the solubility curve and its position in the diagram depends on the degree of agitation of the solution. The three zones are defined as follows:

- I. The stable (undersaturated) zone, where crystallization is not possible
- II. The metastable zone, where spontaneous crystallization is improbable. However, if a seed crystal is placed in such a metastable solution, growth will occur
- III. The unstable or labile (supersaturation) zone, where spontaneous crystallization is more probable.

The achievement of supersaturation is not sufficient to initiate the crystallization. The formation of embryos or nuclei with a number of minute solid particles present in the solution, often termed as centers of crystallization, is a prerequisite. Nucleation may occur spontaneously or it may be induced artificially. Broadly nucleation can be classified into primary and secondary. All types of nucleation, homogeneous or heterogeneous in systems, which do not contain crystalline matter comes under primary. On the other hand, nucleation generated in the vicinity of crystals present in a supersaturated system is termed as secondary.

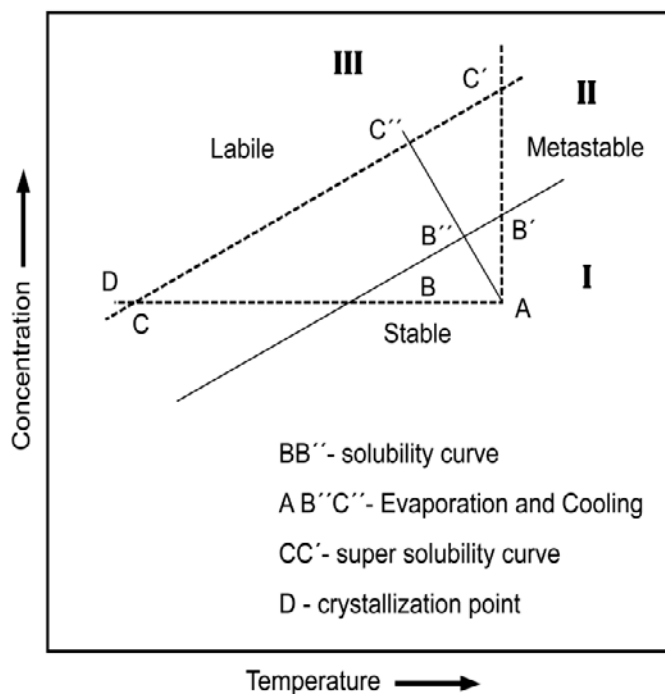


Fig. 1 Meirs and Issac solubility curve

The formation of stable nuclei occurs only by the addition of molecule (A_1), till a critical cluster is formed.



Subsequent additions to the critical cluster result in nucleation followed by growth. The growth units (ions or molecules) in a solution can interact with one another resulting in a short-lived cluster. Short chains may be formed initially or flat monolayers and eventually the lattice structure is built up. This process occurs very rapidly and continues in regions of very high supersaturation. Many nuclei fail to achieve maturity and simply dissolve due to their unstable nature. If the nuclei grow beyond a certain critical size, they become unstable under the average conditions of supersaturation in the bulk of the solution. The formation of a solid particle within a homogeneous solution results from the expenditure of a certain quantity of energy.

The total quantity of work ' W ' required for the formation of a stable nucleus is equal to the sum of the work required to form the surface W_s (a positive quantity) and the work required to form the bulk of the particle W_v (a negative quantity).

$$W = W_s + W_v \quad (5)$$

The change in Gibbs free energy (ΔG) between the crystalline phase and the surrounding mother liquor results in a driving force, which stimulates crystallization. This ΔG is the sum of surface free energy and volume free energy.

$$\Delta G = \Delta G_s + \Delta G_v, \quad (6)$$

For a spherical nucleus

$$\Delta G = 4\pi r^2\gamma + 4/3 \pi r^3\Delta G_v \quad (7)$$

where r is the radius of nucleus, γ is the interfacial tension and ΔG_v is the free energy change per unit volume.

For rapid crystallization, $\Delta G < 0$; the first term in the above equation expresses the formation of new surface and the second term expresses the difference in chemical potential between the crystalline phase (μ) and the surrounding mother liquor (μ_0). At the critical condition, the free energy formation obeys the condition $d\Delta G/dr = 0$. Hence the radius of the critical nucleus is expressed as

$$r^* = 2 \gamma / \Delta G_v \quad (8)$$

The critical free energy barrier

$$\Delta G^* = (16 \pi \gamma^3 v^2)/3(\Delta\mu)^2 \quad (9)$$

The number of molecules in the critical nucleus is given as

$$I^* = 4/3 \pi \gamma (r^*)^3 \quad (10)$$

The crucial parameter between a growing crystal and the surrounding mother liquor is the interfacial tension (γ). This complex parameter can be determined by conducting the nucleation experiments.

Growth of crystals from the vapor, melt or solution occurs only when the medium is supersaturated. The process involves at least two stages [2]:

- (1) formation of stable three-dimensional (3D) nuclei and
- (2) development of the stable 3D nuclei into crystals with well-developed faces.

The formation of 3D nuclei is usually discussed in terms of reduction in the Gibbs free energy of the system. At a given supersaturation and temperature, there is a critical value of the free energy at which 3D nuclei of a critical radius are formed. Only those nuclei which are greater than the critically-sized nucleus are capable of growing into crystals of visible size by the attachment of growth species (i.e. molecules, atoms or ions) at energetically favorable

growth sites like kinks (K) in the ledges (L) of a surface. The surfaces of growing crystals may be flat (F), stepped (S) or kinked (K). However, crystals of visible size are usually bounded by the slowly-growing F faces which grow by the attachment of growth units at energetically favorable sites. Fig. 2 shows different positions for the attachment of growth units at a flat crystal-medium interface of a simple cubic lattice. A growth unit attached at the surface terrace (T), a smooth ledge (L) and a kink site (K) has 1, 2 and 3 out of the 6 nearest neighbors, respectively. Therefore, a growth unit arriving on the surface terrace, at the terrace ledge and at the kink simply loses one, two and three degrees of freedom. If ϕ is the binding energy per pair, the corresponding binding energy of a growth unit attached at these sites is ϕ , 2ϕ and 3ϕ , respectively. Since the probability of capture of a growth unit at a given site depends through terms $\exp(n\phi/kT)$ (where n is the number of bonds formed, k is the Boltzmann constant and T is the temperature in Kelvin), the growth unit has a much higher probability

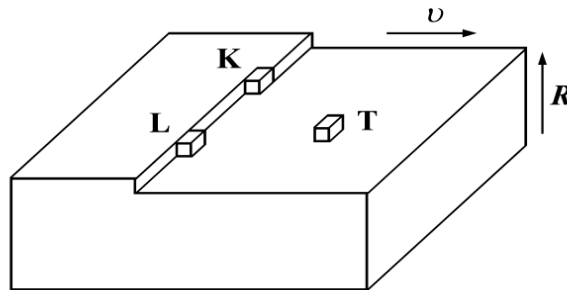


Fig. 2. Different positions for the attachment of growth units at a flat crystal-medium interface of a simple cubic lattice.

of becoming a part of the crystal at the kink site rather than at the ledge or at the surface terrace. Consequently, in contrast to ledges, the contribution of kinks is overwhelmingly high in the rate v of displacement of a step along the surface and in the rate R of displacement of the

surface normal to it. Similarly, the contribution to the face growth rate R by the direct attachment of growth units at the terrace is negligible.

From the above discussion, it may be concluded that the kinetics of crystal growth may, in general, be considered to occur in the following stages:

- (1) Transport of growth units to the growing surface by bulk diffusion and their capture onto the surface terrace.
- (2) Migration of growth units adsorbed onto the terrace to the step by surface diffusion and their capture at the step.
- (3) Migration of growth units adsorbed onto the step to the kink site and their integration into the kink.
- (4) Transport of the released heat of the reaction and solvent molecules from the solvated atoms/molecules.

One or more of the above stages may control the growth rate but the slowest one is always rate limiting. However, it should be noted that growth kinetics, characterized by rates v and R , depends on crystal structure, structure of crystal-medium interface (i.e. rough or smooth), presence of dislocations emerging on the growing face, supersaturation of the growth medium, growth temperature, stirring and impurities present in the growth medium. It is also these factors which ultimately determine the surface morphology of crystals.

To explain the crystal growth processes, various theories and models and role of impurities, have been proposed in the past. Some of them are listed below. For details, one can refer to various excellent references and references therein [2-36]. The important growth models are: (i) Two-dimensional nucleation models; (ii) Spiral growth models; (iii) Bulk diffusion models; and (iv) Growth by a group of cooperating screw dislocations.

2.2 Effects of Convection in Solution Growth

Convection is comprised of two mechanisms: energy transfer due to random molecular motion (diffusion), and energy transferred by the bulk or macroscopic, motion of the fluid. This fluid motion is associated with the fact that, at any instance, large numbers of molecules are moving collectively or as aggregates. Such motion, in the presence of a temperature gradient, contributes to heat transfer. Because the molecules in the aggregate

retain their random motion, the total heat transfer is then due to a superposition of energy transport by the random motion of the molecules and by the bulk motion of the fluid. It is customary to use the term convection when referring to this cumulative transport and the term advection referring to transport due to bulk fluid motion.

2.2.1 Natural Convection

Convection heat flow can be classified as natural (or free) convection and forced convection according to the nature of the fluid flow. Natural convection is due to density difference of a solution near a crystal and far from it. Density difference is due primarily to concentration change of a solution during growth or the dissolution of a crystal; and, secondly, due to the absorption or evolution of the heat in the fluid. In natural convection, fluid motion is due to buoyancy forces within the fluid. Buoyancy is due to the combined presence of a fluid density gradient and a body force that is proportional to density. In practice, the body force is usually the gravitational force. Free convection flows may occur in the form of a plume. The well-known convective flow pattern for solution growth is associated with fluid rising from the bottom of the crystal. During the growth of a crystal, solution rises because the solution near a crystal is less dense as a result of the reduction in the concentration, and the temperature is higher because of the evolution of the heat of crystallization. With this depletion of the heavier solute, the solution around the crystal becomes lighter and, thus, rises. When the crystal is dissolved, the direction of the motion is opposite (downward). Under these conditions, the diffusion of molecules is supplemented by the more energetic convective transport of matter.

Diffusion is the distribution of a substance by a random motion of individual particles. It is due to the presence of a gradient of the chemical potential in the system. A gradient is defined as an incremental of a function in an infinitely short distance, along the direction of the most rapid variation of the function. Diffusion always reduces this gradient. Molecular diffusion is observed in viscous media and at low supersaturations, as well as in the growth of crystals, in thin films of liquids or in capillaries. In molecular diffusion the transport of matter to a crystal is slower than under other diffusion conditions. The thickness of the boundary layer increases with time and the concentration gradient gradually decreases. Therefore, the rate of growth decreases with time. The time interval during the formation of a boundary diffusion layer represents the non-steady state condition. During this initial period,

the rate of growth varies considerably. The thickness of the boundary layer depends on the difference between the densities of different parts of the solution (i.e., on the rate of growth of a crystal), the viscosity of the solution, and the dimensions of the crystal. The presence of the boundary near the crystal and the orientation of the crystal itself affects the nature of the convection currents and the thickness of the boundary layer at different crystal faces.

2.2.2 Forced Convection

Forced convection is produced by the action of external forces such as the forced motion of a crystal in solution. There is no basic difference between forced and natural convection. When the velocity of motion of a solution with respect to a crystal is increased, the thickness of the boundary layer increases and the supply of matter to a face of the crystal increases. Therefore, by increasing the rate of motion of a solution, we can increase the growth rate of the crystal faces. However, we cannot continue this processing indefinitely. A temperature gradient constitutes the driving potential for heat transfer. Similarly, concentration gradient of a species in a mixture (or solution) provides the driving potential of mass transfer. Both conduction heat transfer and mass diffusion are transport processes that originate from molecular activities. Crystal growers are actually concerned with two aspects of the nutrient-to-crystal transport:

- (a) With the mass flux across an interface, which we will call the interfacial flux and which determines the crystal growth rate; and
- (b) With the concentration profile of growth species in the nutrient adjacent to the crystal, which is an essential parameter in morphological stability discussions.

Let us now introduce the dimensionless numbers that govern forced convection and free convection. The Grashof number G_r

$$G_r = \frac{g\beta\Delta T L^3}{\nu^2} \quad (11)$$

where g is gravitational acceleration (m/s^2), (β is thermal expansion coefficient ($\beta = 1/\rho(\delta\rho/\delta T)$ where ρ is density, ΔT is the temperature difference between the horizontal surfaces that are separated by L , and ν is kinematic viscosity (m^2/s). The Grashof number G , plays the same role in free convection that the Reynolds number plays in forced convection. The Reynolds number Re ,

$$Re = VL/\nu = \rho VL/\mu \quad (12)$$

where V is velocity (m/s), L is characteristic length (m), ν is kinematic viscosity (m^2/s), ρ is density, and μ is viscosity ($\text{kg}/\text{s}\cdot\text{m}$). The Reynolds number R_e provides a measure of the ratio of the inertial to viscous forces acting on a fluid element. In contrast, the Grashof number G_r , indicates the ratio of the buoyancy force to the viscous force acting on the fluid.

2.3 Effect of Impurities

We will now define impurities which are inherently present, and additives or dopants which are deliberately added. The former are naturally present in the growth environment and are unwanted; the latter are deliberately added in order to control nucleation, improve crystal quality, increase the size, change the crystal habit and other physical properties. This topic has received great attention since it is of relevant theoretical and practical interest in the growth of crystals of industrial importance. The ability of impurities to change the growth behavior has been studied by many authors [23-36]. It is well known that the influence of impurities on the crystal form and the growth rate is based on the adsorption of the foreign species ions, atoms or molecules at kinks, ledges and terraces of a growing crystal. The change of the crystal form is based on a difference in adsorption energies on different faces. Impurity molecule will be adsorbed preferentially on surfaces where the free adsorption energy has the maximum. It has been possible to predict the preferred surface using computational approaches [37]. Recently the mechanisms and models of adsorption of impurities during the growth of bulk crystals have been surveyed by Sangwal including kinetic effects of impurities on the growth of single crystals from solution [36].

Solvent itself is an impurity. High temperatures and high supersaturations increase growth rate, but in the presence of a solvent the effect of temperature is stronger, since it promotes water desorption and growth kinetics much more than supersaturation, as found for sucrose [38-39]. Anomalies found by Chernov et al., [40] at 10° and 40°C in growth rates disappeared when ethanol, which is known to disrupt the bulk structure of water, was added to the solution. Indeed, water adsorbed on crystal surfaces has properties differing from those of free water. This is attributed to the different structures of the adsorbed layer which undergo phase-like transformations at the above temperatures.

Impurity adsorption can be indirectly studied through the adsorption isotherm, i.e. the fraction θ of adsorbed sites which are occupied as the impurity concentrations C_i

increase. The simplest model of localized adsorption, i.e. situated at lattice sites, is the Langmuir isotherm:

$$K_a C_i = \theta / (1 + \theta), \quad (13)$$

Where K_a is the temperature-dependent adsorption constant, which is different for each crystal face. Other models have been proposed, which take into account the interactions between adsorbed impurities or the occupation probability.

Impurities can act in different ways. When they interact with solute or solvent, they can have strong influences on solubility and consequently on supersaturation and kinetic processes. When impurities are adsorbed on crystals, they can have thermodynamic and kinetic effects. The dominant effect is the exchange rates in which the adsorbed molecule or ions and growth units are involved. If the former are exchanged more rapidly than the latter, adsorption mainly affects surface and edge free energy. For a face a decrease of γ_i (interfacial energy of face i) results, according to the Gibb's equation

$$\Delta\gamma_i = kT \ln(1 - \theta)/S \quad (14)$$

where S is the area of the adsorption site. Similarly, the edge free energy is decreased. These effects should cause an increase in the nucleation and growth rate. If the exchange rate of the adsorbed molecules is slower, impurities can strongly decrease the kinetic coefficients ($R_F = K\sigma^2$ at low supersaturation: $R_F = K'\sigma$ at high supersaturation, where K and K' being kinetic coefficients the value of which depend on temperature and growth mechanisms, R_F is growth rate of F face and σ is the relative supersaturation). So that as a final result the kinetic effects dominate the thermodynamic ones and a decrease in growth rate and impingement flux occur. The interpretation of impurity effects can be done on a structural and kinetic basis:

a) Low concentrations of impurity can form an adsorbed monolayer on the surface even in undersaturated solutions, due to structural relationship between the 2D structure of crystal face and the adsorbed layer (as in the case of NaCl grown in the presence of $CdCl_2$: a monolayer of $Na_2CdCl_2 \cdot 3H_2O$ is formed). The main influence is on the crystal habit.

b) Kinetic interpretation considers the possibility of adsorption on the different surface sites. If impurities are adsorbed in the kinks, the advancement rate of the edge is hindered even at very low impurity concentrations and growth rate is strongly decreased even blocked. Adsorption can also occur on the surface with so strong bonds that impurity

molecules cannot move and form a barrier through which the steps have to filter. The spreading of steps beyond this barrier demands supersaturation higher than a critical value for each impurity concentration. In this case impurities are incorporated. The tailor-made additives are used to modify the crystal habit for industrial needs. The molecules of these impurities are similar to those of crystals, but contain some structural differences, so that when they are incorporated into the crystal they disrupt some bonds and change the growth rate of the faces.

3.0 CLASSIFICATION OF CRYSTAL GROWTH

The methods of growing single crystals may be classified according to their phase transformation as given below:

Growth from solid → solid-solid phase transformation

Growth from liquid → liquid-solid phase transformation

Growth from vapor → vapor-solid phase transformation

One can consider the conversion of the polycrystalline piece of a material into a single crystal by imagining that the grain boundaries are swept through and pushed out of the crystal in the solid-solid growth of crystals. The crystal growth from liquid falls into four categories namely: (i) Melt growth; (ii) Flux growth; (iii) Hydrothermal growth ; and (iv) Low temperature solution growth.

There are number of growth methods in each category. Among the various methods of growing single crystals [41-43], solution growth at low temperature occupies a prominent place owing to its versatility and simplicity. Growth from solution occurs close to equilibrium conditions and hence crystals of high perfection can be grown.

4.0 LOW TEMPERATURE SOLUTION GROWTH

Solution growth is the most widely used method for the growth of crystals, when the starting materials are unstable or decompose at high temperatures. This method demands that the materials must crystallize from solution with prismatic morphology. In general, this method involves seeded growth from a saturated solution. The driving force i.e. the supersaturation is achieved either by temperature lowering or by solvent evaporation. This method is widely used to grow bulk crystals, which have high solubility and have variation in solubility with temperature. After many modifications and

refinements, the process of solution growth now yields good quality crystals for a variety of applications. Growth of crystals from solution at room temperature has many advantages over other growth methods though the rate of crystallization is slow. Since growth is carried out close to room temperature, the structural imperfections in solution grown crystals are relatively low.

4.1 Solution growth methods

Low temperature solution growth can be subdivided into the following categories; (i) slow cooling method; (ii) slow evaporation method; (iii) temperature gradient method ; and (v) Chemical / Gel method

4.1.1 Slow cooling method

Slow cooling is the best way to grow crystals by solution technique. The main disadvantage of slow cooling method is the need to use a narrow range of temperature. The possible range of temperature is usually narrow and hence much of the solute remains in the solution at the end of the growth run. To compensate this effect, large volume of solution is required. Wide range of temperature may not be desirable because the properties of the grown crystal may vary with temperature. Even though this method has technical difficulty of requiring a programmable temperature control, it is widely used with great success. In this method, growth occurs without any secondary nucleation in the solution, if the supersaturation is fixed within the metastable zone limit. A large cooling rate changes the solubility beyond the metastable zone width and multinucleation occurs at the expense of the seed crystal. A balance between the temperature lowering and the growth rate has to be maintained. Growth at a low supersaturation prevents strain and dislocation formation at the interface. Supersaturation can be increased after initial growth to arrive at a reasonable growth rate.

4.1.2 Slow evaporation method

This method is similar to the slow cooling method in terms of the apparatus requirements. The temperature is fixed and provision is made for evaporation. With non-toxic solvents like water, it is permissible to allow evaporation into the atmosphere. Typical growth conditions involve a temperature stabilization of about $\pm 0.05^{\circ}\text{C}$ and rates of evaporation of a few mm^3/h . The evaporation technique has an advantage that the crystals grow at a fixed temperature. But inadequacies of the temperature control

system still have a major effect on the growth rate. This method can effectively be used for materials having very low temperature coefficient of solubility.

4.1.3 Temperature gradient method

This method involves the transport of materials from a hot region containing the solute material to be grown to a cooler region, where the solution is supersaturated and the crystal grows. The main advantages of this method are that

- (i) crystal grows at fixed temperature,
- (ii) insensitivity to changes in temperature provided both the source and growing crystal undergo the same change and
- (iii) economy of solvent and solute.

On the other hand, a small temperature difference between the source and the crystal zones has a large effect on the growth rate.

4.1.4 Chemical / Gel method

The gel method is exceedingly simple. One procedure is to prepare gel using commercial waterglass, adjusted to a specific gravity of 1.06g/cm^3 . Gel is then mixed with 1M tartaric acid and allowed to gel in a test tube. Once gel is formed some other solution can be placed on the top (1M CaCl_2 solution) as shown in Fig. 3 .In due course of time, crystals of calcium tartrate tetrahydrate are formed in the gel. In the nutshell, one solution diffuses through the gel and reacts with other solution to form crystals of appropriate chemicals [44].

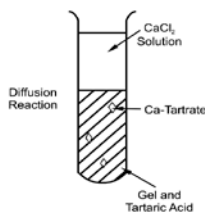


Fig. 3. Schematic diagram of the gel crystal growth process

5.0 SOLUTION GROWTH BY TEMPERATURE LOWERING

The growth of crystals from solution from low temperature solutions occupies a prominent place especially when materials are not stable at elevated temperatures. A number of concepts for solution crystal growth systems are found in literature. One of the best concepts for growth of both inorganic and organic crystals from solution is by temperature lowering of a solution provided the material has positive temperature coefficient of solubility. In this method, a saturated solution of the material to be grown, is prepared at a chosen temperature and kept at this temperature for 24 hours. Then the seed holding rod is inserted in the growth chamber and its rotation is initiated. The growth process is initiated by lowering the temperature slowly. The temperature of the solution is lowered at a pre-programmed rate typically 0.05°C to 2.0°C per day depending on the solubility of the chosen material. The complete crystallization process may take from a week to several weeks. To terminate the growth process the grown crystals are taken out of the solution without thermal shock.

A solution crystal growth is a highly complex process and depends on various growth parameters such as quality of seed, temperature of growth, temperature lowering rate, character of solution, seed rotation and stirring of solution besides other conditions. To grow good quality crystals, the above cited parameters have to be optimized for each crystal.

5.1 Solvent selection and solubility

A solution is a homogeneous mixture of a solute in a solvent. The solute is the component present in a smaller quantity. For a given solute, there may be different solvents. Apart from high purity starting materials, solution growth requires a good solvent. The solvent must be chosen by taking into account the following factors :

- (i) high solubility for the given solute,
- (ii) good solubility gradient,
- (iii) low viscosity,
- (iv) low volatility and
- (v) low corrosion.

If the solubility is too high, it is difficult to grow bulk single crystals and if too small, solubility restricts the size and growth rate of the crystals. Solubility data at various

temperatures is essential to determine the level of supersaturation. Hence, the solubility of the solute in the chosen solvent must be determined before starting the growth process. If the solubility gradient is very small, slow evaporation of the solvent is the other option for crystal growth to maintain supersaturation in the solution. Growth of crystal from solution is mainly a diffusion-controlled process; the medium must be less viscous to enable faster transference of the growth units from the bulk solution to the growth site by diffusion. Hence a solvent with less viscosity is preferable. Most important single crystals such as potassium dihydrogen phosphate (KH_2PO_4) and (L)-arginine phosphate monohydrate (LAP) are grown in aqueous solutions or in solvents that are mixtures of water and miscible organic solvents. Of all known substances, water was the first to be considered for use as a solvent because it is nontoxic, most abundant, and low cost. A proper choice of solvent based on a knowledge of its chemical reactivity helps one to avoid undesired reactions between solute and solvent. Except that, in general, the solubility of the growth materials in solvents is required to be sufficiently large, the solubility parameter δ can often be used in estimating the solubility of nonelectrolytes in organic solvents :

$$\delta = (\Delta U/V_m)^{1/2} = (\Delta H - RT/V_m)^{1/2} \quad (15)$$

where V_m is the molar volume of the solvent, ΔU is the molar energy, and ΔH is the molar enthalpy. δ is a solvent property that measures the work necessary to separate the solvent molecules. Often a mixture of two solvents, one having a δ -value higher than that of a solute and the other lower, is a better solvent than either of the two solvents separately [45]. A selection of δ -values is given in Table 1 .

Another property, that is, the dipole moments between the solute and solvent, may also be considered for selecting solvent for crystal growth. Most typical organic solvents have a dipole moment less than about 3 debye. Therefore, in the case of a solute having a similar value of dipole moment, a much wider choice of solvents is possible.

5.1.1 Solubility determination

Solubility is an important parameter for crystal growth from solution at low temperature. Before any solution growth technique can be applied, determination of congruent or incongruent solubility and the establishment of absence of compound formation with pure or mixed solvents must be achieved. In the latter cases, a special compositional and thermal regime will be necessary to crystallize the desired phase. A

simple apparatus for solubility studies is shown in Fig. 4. Visual inspection allows the determination of the solubility. Upon cooling crystallized material is obtained for solid phase analysis. This apparatus is easily fabricated and is very convenient for measuring solubility. The following is a description of how this has been achieved. The solute and solvent were weighed into a glass ampoule. The ampoule was sealed and rotated in a bath controlled by a thermostat, the temperature of which was increased in steps of 0.5°C every 1-2 h. The final disappearance of the solute yields the saturation temperature. The accuracy of this measurement was within $\pm 0.5^{\circ}\text{C}$.

However, the time needed to reach equilibrium for most covalent organic materials is usually shorter than that of sparingly soluble salts, but the settling times before analyses may be longer. In many soluble salts, such as potassium dihydrogen phosphate, KH_2PO_4 (KDP), triglycine sulfate $(\text{NH}_2\text{CH}_2\text{COOH})_3\text{H}_2\text{SO}_4$ (TGS), and $(\text{CH}_2\text{NH}_2)_2\text{C}_2\text{H}_4\text{O}_6$ (EDT), the solubility is strongly temperature dependent. On the other hand, for some soluble salts, such as LiIO_3 and $\text{Li}_2\text{SO}_4 \cdot \text{H}_2\text{O}$, the solubility is not dependent on temperature and even has inverse slope.

Various techniques for measuring solubility such as methods based on the the vortex flow caused by concentration and optical effects can be found in the literature. However, an accurate measurement of supersaturation is usually difficult. Some new methods such

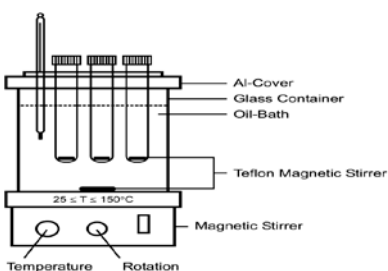


Fig. 4 Apparatus for solubility studies as well as equilibration of feed material and growth solution.

Table I. Solubility Parameters δ of Water and Some Organic Solvents at 25°C

Solvent	δ (MPa ^{1/2})	Solvent	δ (MPa ^{1/2})
Water	47.9	Acetic acid	20.7
Methanol	29.6	1,4-Dioxane	20.5
Ethanol	26.0	Carbon disulfide	20.4
Formamide	39.3	Cyclohexanone	20.3
N-Methylformamide	32.9	Acetone	20.2
1,2-Ethanediol	29.9	1,2-Dichloroethane	20.0
Tetrahydrothiophene-1,1-dioxide	27.4	Chlorobenzene	19.4
N,N-Dimethylformamide	24.8	Chloroform	19.0
Dimethyl sulfoxide	24.5	Benzene	18.8
Acetonitrile	24.3	Ethyl acetate	18.6
1-Butanol	23.3	Tetrahydrofuran	18.6
Cyclohexanol	23.3	Tetrachloromethane	17.6
Pyridine	21.9	Cyclohexane	16.8
t-Butanol	21.7	n-Hexane	14.9
Aniline	21.1	Perfluoro-n-heptane	11.9

as holographic phase-contrast interferometric microphotography and trace fluorescent probe have been developed . Using these techniques, the concentration distributions and thickness of the boundary layers under different convection conditions could be measured with greater accuracy. Although these methods still need more development and refinement to become more generally applicable, they are promising alternatives for determination of supersaturation of easily soluble compounds. Of course, if the solubility is known, supersaturation can be calculated by measuring the temperature of the solution and its equilibrium temperature. The problem is that equilibrium temperature measurements are not always easy.

5.2 Design of a Crystallizer

When designing crystallizer for growing crystals from solution by the temperature lowering method, the following conditions should be met [43, 46-47]:

- (i) The range of operating temperature from room temperature to 80°C, depending on the solvent.
- (ii) The choice of hydrodynamic conditions in the solution.
- (iii) Measurements of growth parameters such a growth rate.
- (iv) The arrangement of the taking out the grown crystals from the crystallizer without any thermal shock.
- (v) The arrangement of changing the saturation/temperature decrease rate.
- (vi) The possibility of changing the different kind of seed holders.
- (vii) The long term operating reliability of the system.

Since these types of solution crystallizers are not available in the market, one has to design and fabricate ones' own system based on ones requirements. A description of a modified crystallizer for growing large crystals from solutions along with the design of a versatile electronic reciprocating control system to change and reciprocate the motor speed containing the seed holding rod for solution growth crystallizer is given below.

In this system, the rotation rate and number of revolutions in the clockwise and counter clockwise direction can be adjusted as desired. This electronic system alleviates the problem of jerky motion the of seed holder [56] during reciprocation as in earlier electro-mechanical systems designed by the authors. Good quality crystals of important nonlinear optical materials such as Methyl-(2,4-dinitropheny)-aminopropanoate: 2-Methyl-4-

nitroaniline (MNA:MAP), L-Arginine Phosphate (LAP) L-Histidine tetrafluoroborate (LHFB), L-Arginine tetrafluoroborate (LAFB) and others such as triglycine sulfate, potassium dihydrogen sulfate have been successfully grown in authors' laboratory using this system [47-53]. The complete crystallization apparatus along with electronic circuit can be easily fabricated in the laboratory with readily available components.

5.2.1 A Typical Solution Crystal Growth Crystallizer

A schematic diagram of a modified solution crystal growth systems that the authors designed and fabricated after designing a number of crystallizers [55-58] in our laboratory is shown in Fig.5. It consists of a 250 ml crystallizer jar (4), which holds the growth solution, that is placed inside a 2.5 liter glass jacketed kettle (2). The linear and reciprocating motion of the Teflon seed holder (5) is controlled by a rack-pinion arrangement (8) and electronic circuit (7) respectively. A reversible motor (6) is used for rotating the seed holder. The temperature of the growth solution is controlled and programmed by circulating water using a NesLab bath (1). To prevent evaporation of the solvent, a specially designed oil Teflon seal (3) and/or RTV/Teflon seal (3) are used. The main advantages of our crystal growth system are: (i) better temperature stability even with sudden fluctuations in room temperature, (ii) better control over evaporation of organic solvents, (iii) a mechanical screw type arrangement for pulling the seed crystal at a controlled rate, (iv) the possibility of varying the seed orientation and type, and (v) a versatile electronic reciprocating control system to change and reciprocate the motor speed containing the seed holding rod. Better temperature stability was accomplished by loading the growth solution in a beaker kept inside the jacketed vessel.

An air gap provides extra insulation. Moreover, spontaneous nucleation at the bottom of the growth vessel, which hampers the growth and the crystal yield, is completely eliminated. By providing an extra lid on the inside beaker and a Teflon seal over the jacketed vessel, the evaporation of the solvent was reduced dramatically. The inner beaker is filled halfway with solution rather than three-fourth as usually done and the growing crystal is pulled in a controlled fashion. Since filling of the inner beaker, to three-fourth, is not required, not only the crystal is annealed in situ but also spurious aloevera-tree like growth near the seed in some crystals such as MNA:MAP, is greatly reduced or completely eliminated.

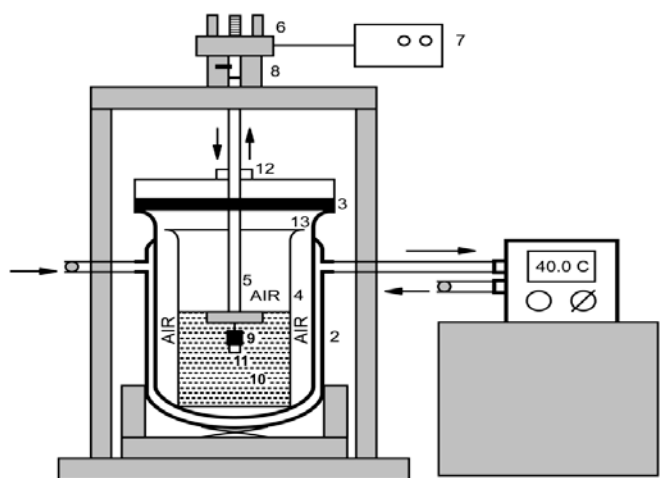


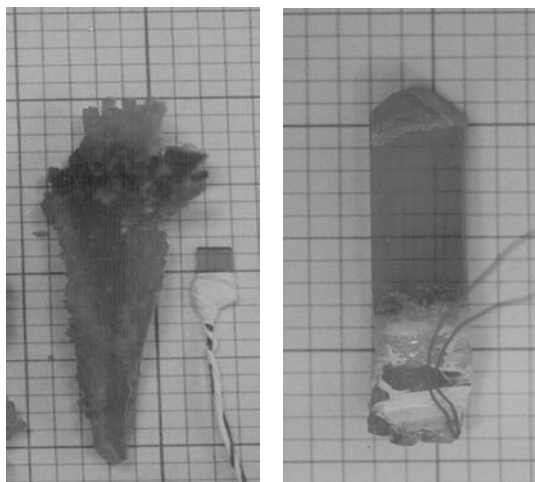
Fig. 5. Schematic diagram of a new type of crystallizer for growing organic crystals.

(1) Circulating bath; (2) Jacked reaction kettle; (3) RTV/Teflon seal; (4) Crystallizer jar; (5) Teflon seed holder; (6) Reversible motor; (7) Circuit for reciprocating and controlling the stirring rate of seed holder; (8) Arrangement for pulling the crystal during growth; (9) Teflon tape cover; (10) Solution; (11) Seed crystal; (12) Teflon seal; (13) Glass lid.

Fig. 6 (a) shows the seed crystal along with a MNA:MAP crystal grown using usual technique i.e. without pulling the growing crystal. Fig. 6(b) shows the same crystal grown with pulling where aloevera-tree type growth is avoided. Furthermore, large crystals can be grown from a smaller amount of expensive mother liquor when the crystal is pulled while growing.

Another modified solution growth crystallizer was also designed in our laboratory, whose three dimensional cutout view with reciprocating seed arrangement and other components is illustrated in Fig. 7. It uses magnetic stirrer to keep the temperature of the water bath uniform at a particular temperature. A layer of silicon oil on the surface of water was found to reduce the evaporation of water to a minimum which is a big improvement over earlier designs.

Besides temperature control, the uniform rotation of seeds is required so that stagnant regions or re-circulating flows are not produced, otherwise inclusions in the crystals will be formed. To study and achieve uniform and optimum transport of solute to the growing crystals, various seed rotation mechanisms have been used in the past. The unidirectional rotation of the seed leads to the formation of cavities in central regions of a crystal face because of lesser solute transport to this region than edges and corner of the growing crystal. Furthermore, non-uniform solute supply favors the formation of



(a)

(b)

Fig. 6 The Photographs of MNA:MAP seed and (a) aloevera-tree type growth (b), without aloevera-tree type growth

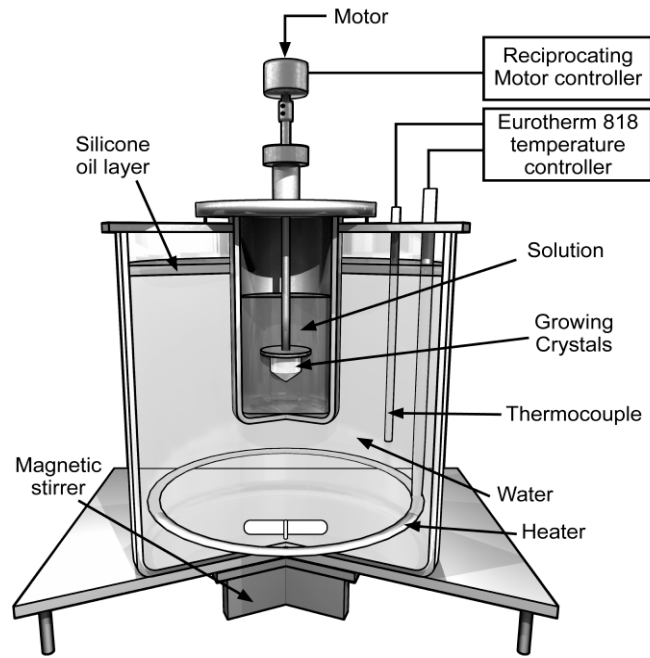


Fig. 7 A Modified crystallizer with arrangement to stop water evaporation

thick layers which subsequently lead to the trapping of inclusions and the generation of dislocations. Periodic rotation of the growing crystal in opposite directions suppresses edge formation but does not eliminate the formation of the central cavity. To avoid these defects and stagnant regions in the solution, eccentric or clock-wise and counter clockwise motion of the seed holder is used in growing crystals from solutions. A few mechanisms [54-56] have been used in the past to generate reciprocating motion of the seed holder such as electro-mechanical [55] and rack-pinion [56]. In the electro-mechanical system, a connection of the motor polarity is reversed mechanically by using

a micro-switch. In this mechanical system, there is a jerky motion on reversal, which sometimes causes seeds to fall down. The jerky motion also creates a turbulent flow in the fluid and hence non-uniform transfer of solute to the growing faces, thereby defective crystals may be formed. The micro-switch has to be changed frequently due to mechanical failure. Furthermore, the effect of seed rotation rates on the growth rate and the quality of the crystals can not be systematically studied because rotation rate cannot be varied. In the rack-pinion arrangement, there is no jerking motion but one has to change gears to change rotation and reversal rate, which is quite an involved process.

To improve on these drawbacks, in our Crystal Growth Laboratory at Alabama A&M University, a versatile solid state electronic circuit for reciprocating the direction of the seed holder was designed along with added features in such a way as to vary rotation rate, stopping time on reversal, and controlled timing for clockwise and counter clockwise motion of the crystal/seed holder [57]. These designed features will allow the crystal growers to study more decisively the effect of seed rotation rates on the growth and quality of the grown crystals, thereby optimizing this important parameter for growing better quality crystals.

A schematic diagram of the basic electronic circuit for reciprocating motion control is shown in Fig.8. In Fig.8, the timer (Chip LM 555, U3) produces a square wave timing pulse. It may be set for a particular frequency (POT1) and duty cycle (POT2) in combination with timing capacitor (C3), and reset if necessary by switch (S2). The timing wave form is divided by the J-K flip flop chip 74LS112 (U1) to one half the timer frequency. Parasitic oscillations are suppressed by capacitors (C1, C2 and C4). The two wave forms are combined by NAND gates chip SN7400 (U2) to alternately turn on the transistor (Q1 and Q2) to control the solid state relays (1 and 2) which connect the alternate sides of the motor capacitor to the 110 VAC return line. Similarly, the transistor (Q3 and Q4) alternately turn on the indicator lamps (LED1 and LED2). Current limiting and bias is provided by resistors (R1 through R8). Motor rotation speed is controlled by potentiometer (POT3). A power supply consisting of the step down transformer (T1), voltage regulator (U4) and associated filtering circuit (D1 and D2, C5 and C5), and voltage setting divider (R9 and R10) provides 5 VDC to the circuit. The

operation of the circuit causes the following sequence of states in the system: during first interval, the seed holder motor runs counter clockwise; during the second interval,

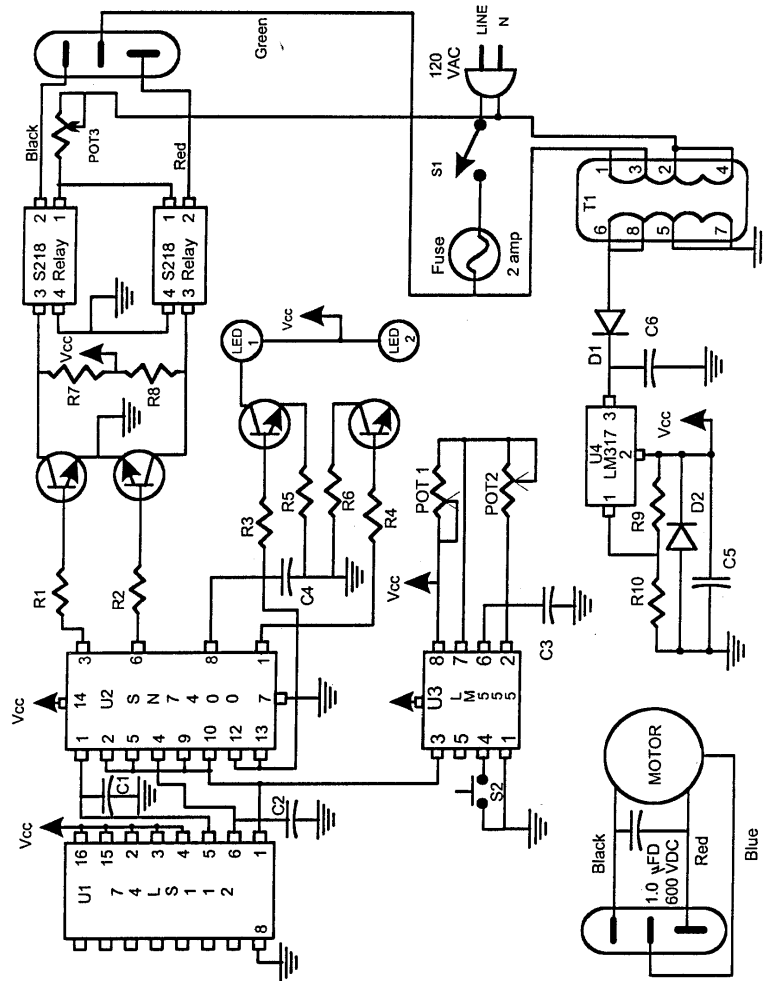


Fig. 8 The Electronic circuit diagram for reciprocating motion of seed holder for solution crystallizer

the motor comes to a stop; during third interval, the motor runs clock wise; and during the fourth interval, the motor again comes to stop. Then the entire cycle of operation in repeated, and the intervals can be varied as needed for a particular crystal growth experiment.

5.2.2 Crystal Seed-Holder

In order to insure the best growth conditions, it is necessary to use a special crystal holder because the success of an experiment may depend upon its suitability. The selection of the crystal holder and the method for attaching a seed to it are no less important than the selection of the growth method. A crystal holder should insure that a seed is held securely in a desired orientation and that the seed and therefore the growing crystal can be moved in any required manner. Also, the crystal holder should not become deformed at the selected speed and direction of the motion or by the weight of the final crystal grown on it. The crystal holder material should be chemically inert in the solution of the substance being crystallized.

The schematic diagram of two plexiglas seed holders were specially designed, fabricated, and successfully used by the authors for aqueous solution crystal growth are shown in Fig. 9.

5.2.3 Preparation of seed crystal and mounting

A seed is small fragment of a crystal or a whole crystal which is used to start the

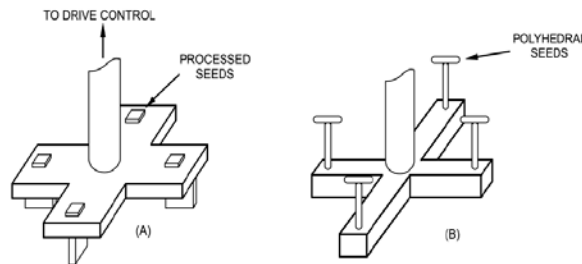


Fig. 9 Plexiglas seed holders for solution growth crystallizers

growth of a larger crystal in a solution. This seed must meet the following requirements:

- (i) It should be a single crystal free of cracks or boundaries,
- (ii) It should be free of inclusions

- (iii) Its surface should be free of any sharp cleaved edges
- (iv) It must be grown under the same conditions as those to be used in

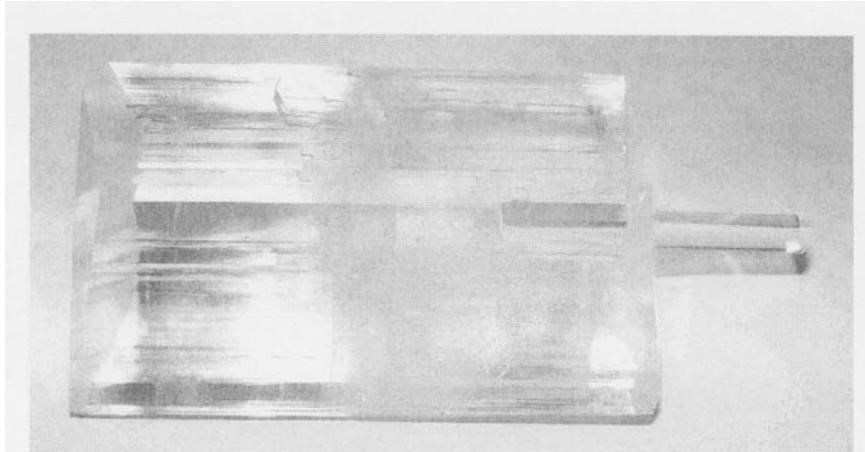
growing the desired single crystals. Following the above requirements in preparing the seed crystals will result in the growth of high quality crystals, if other criteria such as solution preparation etc., are performed carefully as well. Prior to crystal growth, seed crystals are mounted on plexiglas rods using 100% silicon rubber Dow Corning Silastic 732 RTV adhesive.

5.3 Solution Preparation and Starting a Growth Run

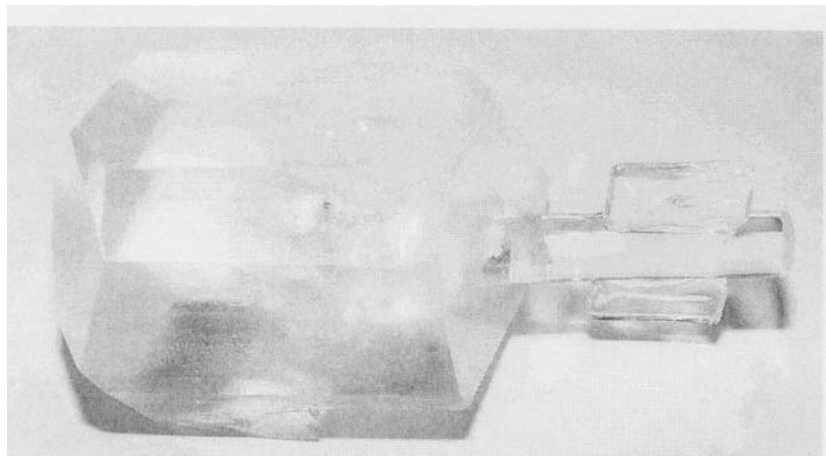
For solution preparation it is essential to have the solubility data of the growth material at different temperatures. Sintered glass filters of different pore sizes are used for solution filtration. The clear solution, saturated at the desired temperature is poured into the growth vessel. For growth by slow cooling, the vessel is sealed to prevent solvent evaporation. Before starting the crystal growth process, a small crystal suspended in the solution is used to test the saturation. By varying the temperature, a situation is obtained where neither growth nor dissolution occurs. The test seed is replaced with a good quality seed. All unwanted nuclei and the surface damage on the seed are removed by dissolving at a temperature above the saturation point. Growth is initiated after lowering the temperature to the equilibrium saturation. A controlled solvent evaporation can also be used in initiating the growth. The quality of the grown crystal depends on the a) nature of the seed, b) cooling rate employed and c) agitation of the solution.

Various new nonlinear optical crystals which holds promise for their use in optical processing devices such as L-arginine phosphate, L-Histidine tetrafluoroborate, L-arginine tetrafluoro borate, Methyl-(2,4-dinitropheny)-aminopropanoate: 2-Methyl-4-nitroaniline (MNA:MAP) and L-pyroglutamic acid have been successfully grown using the above mentioned reciprocating system in combination with temperature lowering technique described by the authors [47-50]. Some of these crystals are shown in Fig. 10. In the investigators' observation and experience, there is significant improvement in the quality of grown crystals and success rates of the growth runs, which is evident from the transparency and less scattering that is observed using laser illumination. This reciprocal

motion control electronic system for the solution growth crystallizers has been in use in our laboratory for several years, and continues working satisfactorily.



(a)



(b)

Fig. 10 Photograph of crystals grown at Alabama A&M University (a) L-Histidine tetrafluoroborate (b) L-pyroglutamic acid crystals

It is worthwhile to mention that this simple and versatile crystallization apparatus can be fabricated in any college, university, or scientific laboratory from readily available components. Besides its use in physics or chemistry laboratory experiments, it can also

be used for doing extensive research on the effect of important parameters such as seed rotation rate, stopping time of reversal, and number of rotation in the clockwise or counter clockwise direction on the quality and growth rate of technologically important crystals.

6.0 TRIGLYCINE SULFATE CRYSTAL GROWTH– a case study

Triglycine sulfate (TGS) is one of the most important ferroelectric materials. The ferroelectric nature of triglycine sulfate, $(\text{NH}_2\text{CH}_2\text{COOH})_3\cdot\text{H}_2\text{SO}_4$, usually abbreviated as TGS, was discovered by Matthias, Miller and Remeika and discussed by Jana and Shirane [59]. The crystal structure of TGS was reported by Hoshino, Okaya and Pepinsky and discussed in above reference. In the ferroelectric phase below the Curie temperature ($T_c \sim 49^\circ\text{C}$), the symmetry is monoclinic with space group $P2_1$. Above the Curie temperature, the structure gains an additional set of mirror planes in the space group $P2_1/m$. It has been reported that $a = 9.42 \text{ \AA}$, $b = 12.64 \text{ \AA}$; $c = 5.73 \text{ \AA}$; $\beta = 110^\circ 23'$ and that the structure contains three independent glycine molecules. One of the structures designated as glycine II, has a zwitter-ion configuration $(\text{NH}_3)^+\text{CH}_2\text{OO}^-$, and the other two, $(\text{NH}_3)^+\text{CH}_2\text{COOH}$. The TGS may be called glycine-diglycinium sulfate with chemical formula $((\text{NH}_3)^+\text{CH}_2\text{COO}^-)\cdot((\text{NH}_3^+)\text{CH}_2\text{COOH})_2\cdot\text{SO}_4^{2-}$. The projection of the structure along the c-direction is illustrated in Fig. 11. Glycine I deviates only slightly from the plane m' at $y = 1/4$ on which the $[\text{SO}_4]^{2-}$ tetrahedra also lie, whereas glycine II and III are approximately related by inversion through $(1/2, 1/2, 1/2)$ [60].

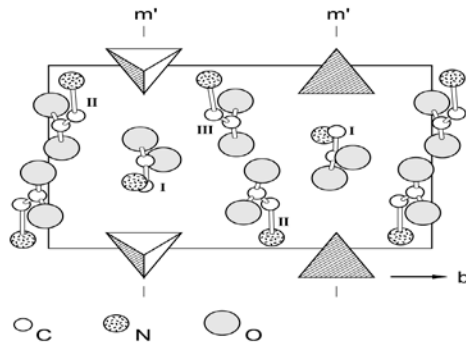


Fig. 11. The projection of the structure of TGS crystal along c-direction: m' represents the set of pseudo mirror planes in which glycine I molecules are inverted on ferroelectric switching.

6.1 Growth of Single Crystals of Triglycine Sulfate

Single crystals of TGS have been usually grown from aqueous solution by the temperature lowering or solvent evaporation method. The authors have successfully grown the TGS crystals using the crystallizer illustrated by the schematic diagram shown in Fig. 12 [58]. The outside water bath, with a capacity of about 12 liters, and the inside smaller cubical growth cell with 1 liter capacity were made out of Plexiglas. Temperature control of the crystallizer was achieved using a 250-W immersion heaters controlled by YSI 72 proportional temperature controllers to an accuracy of $\pm 0.1^\circ\text{C}$. The uniformity of the temperature throughout the bath was achieved with the help of fluid circulation pump. The bath temperature is monitored at two points during the crystal growth using NBS calibrated thermometers. The crystals were grown by slow cooling of the solution at any desired rate.

TGS crystals are doped with L-alanine to enhance its performance and check depoling for their use in infrared sensor element. A rotating disc technique [61] has been applied to grow uniformly L-alanine-doped TGS crystals using a large area seed crystal having large (010) face. A conventional crystallizer was modified to allow growth under suitable hydrodynamic conditions in order to stabilize growth on the (010) face. Such a crystallizer is shown in Fig. 13. In this crystallizer, a seed crystal in the form of a disc was held in a circular holder with the (010) face exposed to the solution. The disc was attached to the end of a spindle that was rotated at 340 rpm. This creates a uniform boundary layer of solution over the crystal's exposed face. The container with a 30 liter capacity was heated by a hot plate spaced from its bottom surface and regulated to hold the temperature with in $\pm 0.01^\circ\text{C}$. The solution rises from the bottom of the vessel but hotter liquid is prevented from reaching the crystal directly by a plexiglas baffle. A growth rate of 1mm/day was maintained by lowering the temperature uniformity at $0.05^\circ\text{C}/\text{day}$. The resulting crystals were found to be visibly of good quality, without

defects propagating from the seed. In addition to uniform doping and growth of high quality crystal, the method has several other useful features such as short growth time,

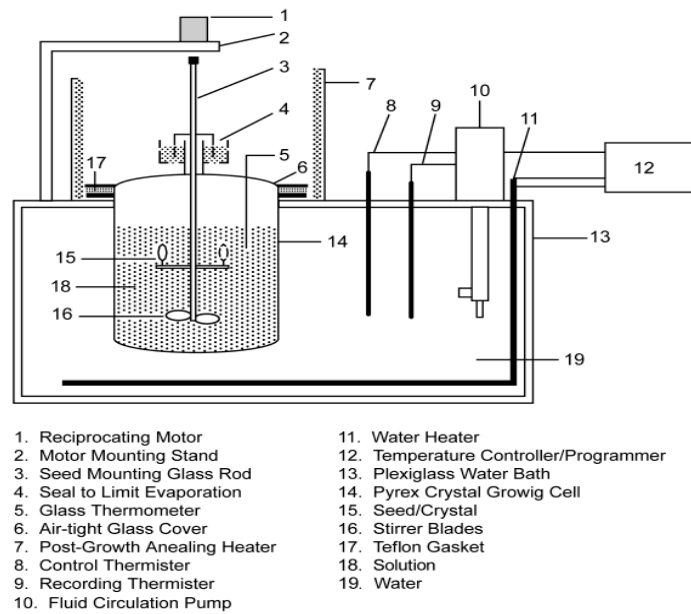


Fig. 12 Schematic diagram of reciprocating motion crystallizer.

with decrease cost and re-use of seeds, and growth occurs within a small temperature range. Brezina et. al., [62] designed a crystallizer for growing L-alanine doped deuterated triglycine sulfate (DTGS) crystals by isothermal evaporation of D₂O.

Satapathy et. al., [63] have described a novel technique for mounting the TGS seeds and a crystallizer.

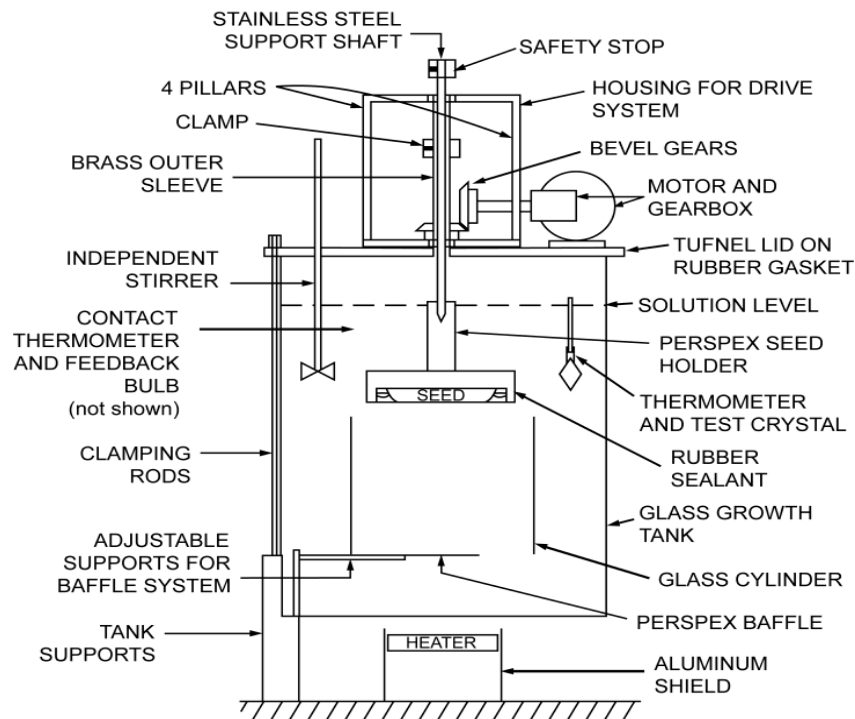


Fig. 13 Apparatus for spinning disc growth.

Banan [64] has also described a crystallizer and a seed holders for growing pure and doped TGS crystals.

TGS crystals weighing more than 100 grams have been grown from solution with ethyl alcohol additions [65]. When alcohol is mixed in an aqueous solution of TGS, part

of the water in the solution associates with alcohol, which concentrates the solution. Thus, the supersaturation can be controlled to a certain degree, making it easier to grow TGS crystals.

To achieve success in the growing crystals from aqueous solutions, it is important to prepare a solution with a well determined saturation temperature, solubility profile, and absence of any foreign particles. For our investigation, TGS solution was prepared using high purity crystalline triglycine sulfate by BDH, UK. The solubility of TGS at various temperature were determined and compared with information available from various sources. TGS solution was prepared at 40° C saturation temperature. To prepare saturated solution, 464 grams of TGS was weighed and dissolved in 1000cc of distilled water. The mixture was heated to 50°C, and mixed thoroughly using a Teflon coated magnetic stirrer. The solution was then filtered through a 5 micron filter funnel using a vacuum unit. After filtration, this solution was transferred into the growth chamber. To start the growth run, the bath temperature was kept at 45°C. The solution was poured into the growth cell. Then the temperature was reduced to 41.5 °C, 1.5 degree above the saturation temperature, and was allowed to stabilize over night. The saturation temperature was again checked by crystal insertion into the solution technique, and also refractive index measurements. For each saturation point the refractive index was measured at different temperature before hand using Abbe refractometer. The starting growth temperature was adjusted based on the result of this procedure. After this the seed crystal-holder was placed in an oven and heated upto 45°C. Prior to transferring to the growth cell, All precautions were taken to keep the seeds as well as the holder surface free of dust or foreign particles. The preheated seed crystals holder were then inserted into the growth cell and holder attached to the reciprocating apparatus. The seed crystals were slightly dissolved and the growth run started. The bath temperature was reduced by 0.1°C /day initially and at final stage of growth by 0.2 C/day. The removal of the grown crystals from mother liquor requires some care. Mishandling may induce defects thus destroying the scientific value of the crystal or even fracture it all together. To avoid cracking the crystals due to thermal shock, the crystals were wrapped in a lint-free paper towel maintained at final growth temperature. The crystals were then transferred to an oven kept at an appropriate temperature. The temperature of the oven was slowly lowered to room

temperature. Grown crystals can be easily removed from the seed holder by the slight force by fingers as RTV 732 adhesive was used for mounting the seed crystal

6.2. GROWTH KINETICS AND HABIT MODIFICATION

Triglycine sulfate normally grows with the habit shown in Fig. 14. It is observed that the growth rate $V_{(010)}$ is much faster than $V_{(001)}$. So the (010) face as seen in Fig. 14 is very small or not present. Both growth kinetics and habit modifications of TGS have been extensively studied over the past several decades. The work published so far has resulted in a description sufficient for reliable growth of this crystal as described in the previous section. A number of studies of the growth kinetics of TGS grown from aqueous solution have been reported in the literature [66-71]. Novotny and Moravec [69] studied the growth of the (110) face of TGS crystals grown isothermally above the phase transition, at higher supersaturation ($\sigma > 10^{-3}$) and under constant hydro-dynamically controlled conditions. The researchers observed that the ratio of growth rates along the individual axes is $V_a:V_b:V_c = 0.67:1:0.25$. On the basis of the measured dependence of the linear growth rate upon the supersaturation (σ), it was found that the growth of the (110) face is probably controlled by volume diffusion of TGS molecules towards the surface of the growing crystal. Increasing supersaturation caused a reduction of the number of faces in the prismatic zone of the crystal and an increase of the dislocation density in the (110) faces. Measurements of the growth rates [69] of (110) and (001) faces as a function of supersaturation of the solution were also analyzed on the basis of the

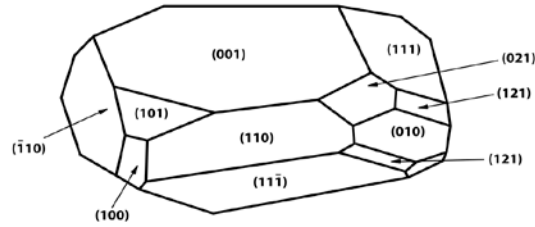


Fig. 14 Normal growth habit of TGS crystal.

surface-diffusion model of Burton, Cabrera, and Frank (BCF) [67]. It was shown that surface diffusion is responsible for the low growth rates of (001) faces; in the case of (110) faces, the mechanism is less important at higher values of supersaturation than volume diffusion. Rashkovich [68] investigated the growth of (001) faces below the transition temperature. The results were qualitatively consistent with the dislocation model of crystal growth, but the growth at low supersaturation did not agree with the BCF model [67]. Reiss et al., [71] studied the growth of crystals at 33.55°C at relative supersaturations of 0.004 and 0.045. In their study, both BCF and Birth of Spreading growth laws are fitted to the growth rate data. They also found that qualitative aspects of the growth are consistent with the BCF model.

The role of pH, impurities, degree of supersaturation, growth temperature and technical parameters, including seed preparation and attachment, etc., on growth kinetics has also been quantitatively investigated by various investigators [72-90]. The results are described in following section.

6.2.1 Effect of Seed Crystal

It has been observed that morphology does not change much for seed crystals obtained at different temperatures [79]. However, at higher temperatures (35-45°C) seeds tend to be elongated in the (001) direction, while seeds grown at lower temperatures are nearly isometric. Morphological study of the crystals

grown using the above cited seeds showed the dependency of the crystal habit on the characteristics of the seed. The grown crystals tended to be elongated when the elongated seeds were used. Crystals with large size (010) faces grew when cleaved platelets were used for seeding. Crystals with high transparency and lower dislocation densities were obtained when the crystal growth-temperature was kept the same as that used to grow the seed. Crystal growth was seriously impaired when cleaved platelets were used as seeds because of unwanted nucleation that started growing during the growth process. Banan et al., [81] studied the effect of using poled seed on the morphology and growth rate of TGS crystals. Table 2 summarizes the normalized growth data for two crystal growth runs using poled and unpoled seeds, and Fig. 15 gives the morphology of resulting TGS crystals. A number of interesting effects on the growth rate and morphology of these crystals were observed. Generally, the growth rate along the (-b-axis) (010) was faster than along (010) (+b-axis). The well developed (010)/ $0\bar{1}0$ faces, which are generally not present or less developed in pure TGS crystals, were prominent and large in crystals grown on poled seed. In this way, the identification of the ferroelectric axis in the TGS crystal becomes easier, and cleaving normal to the ferroelectric axis for preparation of pyroelectric IR element can be economically accomplished. It can be inferred from Table 2 that growth velocity along [010] axis of TGS crystal is affected by using a poled seed crystal. The decrease in growth rate along [010] direction in the case of poled seed helps in the emergence of larger (010) face.

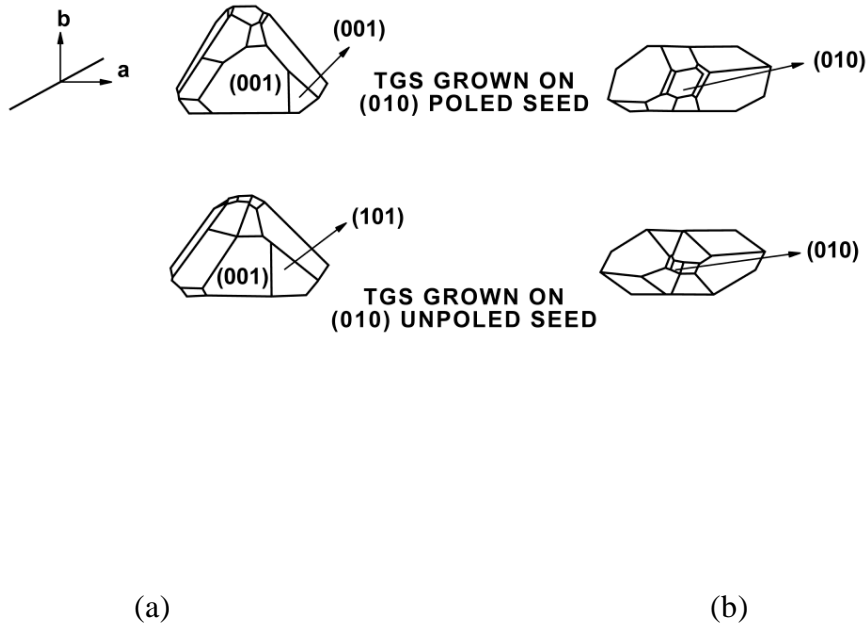


Fig. 15. Growth habits of TGS crystals grown on (a) poled and (b) unpoled seeds.

6.2.2 Effect of Growth Temperature and Supersaturation

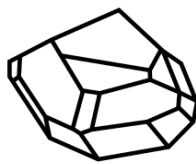
The dependency of crystal morphology and quality on growth temperature using seed obtained from the growth solution and at the crystal growth temperature has also been studied [79]. The change in the morphology was not substantial, but the rate of growth in different directions changed with the temperature, and relative change in the size of the faces was observed. Extra nuclei hindered the growth at higher temperature (40°C), and the crystals were of poor quality with low transparency. The change in habit of TGS crystals [75] as a function of temperature and supersaturation is shown in Fig. 16.

Table 2 Crystal growth data for TGS crystals grown on poled and unpoled seeds

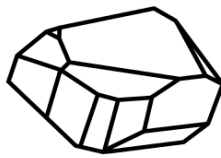
TGS Crystals	crystal yield wt (g/day °C)	Growth velocity, $V_{(010)}$ (mm/day °C)
(010) poled seed	0.618	1.05
(010)unpoled seed	0.621	1.16
(0 $\bar{1}$ 0) poled seed	0.624	1.20
(0 $\bar{1}$ 0)unpoled seed	0.637	1.25

6.2.3 Effect of pH of the Solution

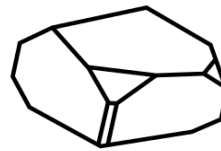
The influence of solution pH on the growth, morphology, and quality of TGS crystals has been studied by a number of workers. It was observed that crystal quality is not much affected by pH variation [79]. The influence of growth solution pH on growth rates of various faces: {(001), (010), (100)} and habit of TGS was studied by Tsedrik *et al.* [75].



a



b



c

Fig 16 Change of growth habits of TGS with growth temperature and supersaturation (a) 32°C, 0.7×10^{-3} (b) 32°C, 3.0×10^{-3} and (c) 52°C, 3.0×10^{-3} .

At a $\text{pH} < 1$, diglycine sulfate (DGS) was formed. Table 3 gives the values of average growth rate V of (001), (010) and (100) faces of TGS crystals vs. pH of the solution as well as DGS grown at pH 0.3. Values for $V_{(100)}$ decreased monotonously with the lowering of pH , and, $V_{(001)}$ and $V_{(100)}$ had a local minima near the pH value corresponding to the stoichiometric ($\text{pH} = 2.14$) value and a local maxima around $\text{pH} = 1.25$. The crystal habit is defined by the growth rates of the faces. Fig. 17 shows the dependence of crystal habit on pH [75]. The most isometric crystals were obtained at $\text{pH} = 1.55$, when $V_{(100/001)} \sim 1$ (Fig. 17(c)). Almost all crystals at low pH had gaps on the (111) and (111) faces (Fig. 17(d) and (e)). The above observed changes in morphology of TGS single crystals with the pH of the solution were apparently affected by different capture of incidental impurities, which are always present in the solutions. Chemical (structural) impurities captured with the crystal faces reduced the growth rates of corresponding faces, and mechanical impurities (defects) increased the above mentioned rates. At low pH values, chemical impurities played the predominant role. Their entry into the growing crystal was increased with reducing pH . Table 3 clearly shows that the growth rate of all faces decreased with reducing pH , starting with $\text{pH} = 1.25$. The gaps on (111) and (111) faces were connected with strong hindering of the growth layers by the absorbed impurities (Fig. 17 (d) and 17(e)). At high pH (>2) another kind of impurity (mechanical defects) has a predominant influence on crystal morphology. Their entry increased with rising pH . So that the growth rates of all faces increased (Table 3). At $\text{pH} = 1.55$ the action of impurities of both kinds was comparable, and mostly isometric crystals were formed (Figure 17(c)). Recently, it has been shown [97] that the growth rate of (010) face of TGS and ATGSP crystals varies with pH the of the solution.

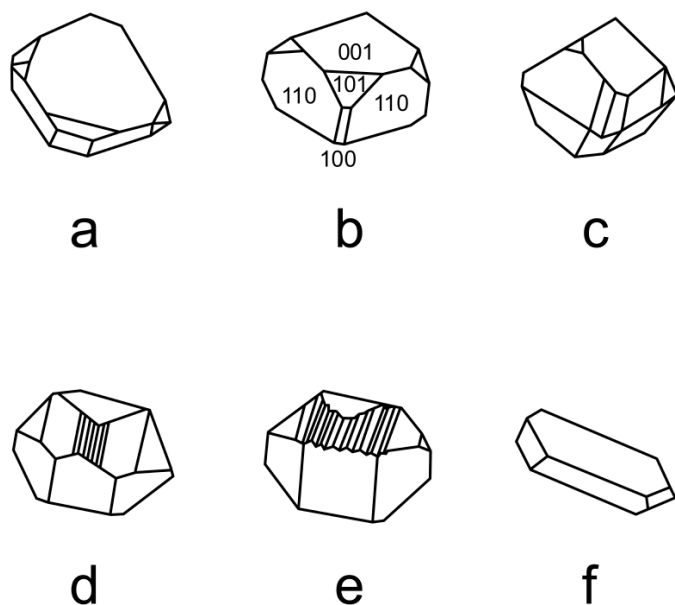


Fig. 17 Change of habit of TGS crystals with pH of the solution (a) 2.75, (b) 2.1, (c) 1.55, (d) 1.23, (e) 1.0. and (f) 0.3 (DGS)

Table 3 Growth rates of various faces of TGS vs. pH of solution [75]

pH	$V_{(001)}$ (10^3 mm/hr)	$V_{(010)}$ (10^3 mm/hr)	$V_{(100)}$ (10^3 mm/hr)
2.70	71.6	291.5	260.9
2.14	49.6	118.2	117.6
1.25	207.0	262.0	109.0
1.00	144.6	156.2	43.9
0.30	109.9	120.9	40.5

with the same supersaturation, the growth rate of TGS crystals was the slowest in the neutral solution (pH = 2.25). It grew faster both in acidic solution (pH = 1.73-2.25) and

alkaline solution (pH = 2.25-2.52). In alkaline solution, the growth rate of TGS varied faster with the change of pH value. However, if the pH was too high, then the (010) face capped quickly. The variation of growth rate of L-alanine doped triglycine sulfo-phosphate (ATGSP) with pH was not similar to that of TGS. The growth rate of ATGSP crystals in a neutral solution (pH = 2.5) was the fastest, and it was slower both in acidic (pH = 2.20-2.50) and alkaline (pH = 2.5-2.85) solutions. The above results demonstrate that on the basis of the pH of a solution, one can grow crystals at higher growth rates.

6.2.4 Effect of Impurities on TGS crystal growth

The presence of impurities in the process of crystal growth results in modification of the crystal shape and growth rates. Different workers have studied the effects on the kinetics of growth of doping TGS crystals with inorganic and organic impurities. It was observed that Ni-doped crystals were very similar in habit to pure TGS crystals, while in the case of Cu- and Fe-doped crystals, the numbers of developed faces were strongly reduced [70]. In the presence of Ni-, Co- and Cu-ions, the rate of crystallization decreased [80]. An odd behavior was found while growing Cr-doped crystals. The addition of Cr- with a concentration of 1 % changed the regime of crystallization owing to the high chemical activity of these ions. At a concentration of about 3%, the rate of crystallization became very fast even without lowering the temperature [80]. In Pd-doped crystals, the ratios of the growth rate along the c-axis to the growth rate along the a and b axes slightly decreased as the crystal grew larger [85]. For medium size crystals (~30 g), the average relative growth rate along the c-axis was larger by more than an order of magnitude in Pd-doped crystals than in pure TGS. Pd-doped crystals also developed other faces which have not been observed before. Banan et al. [81] studied the effect of Ce-, Cs-, L-alanine and L-alanine + Cs on the growth and morphology of TGS crystals. Table 4 shows the crystal growth data, and Fig. 17 shows their habit. The well-developed (010)/(0 $\bar{1}$ 0) faces, which were generally not present or less developed in pure TGS crystals are obtained with L-alanine or Cs doped crystals. Moreover, (101) faces obtained in crystals doped with L-alanine and in crystals doped with Cs and L-alanine were more dominant than pure TGS crystals. Also, the axial velocities, $V_{(001)}$ and $V_{(100)}$, were affected by doping (Table 4). Lower

growth rates were especially obvious in Cs doped crystals. The crystals became plate-like for $V_{(010)}/V_{(001)} \sim 28.0$; and the habits was strongly disturbed (Fig. 18). L-alanine doped crystals developed a habit which was asymmetric about (010) plane. The growth rate in the positive b direction was higher than in the negative b direction [29].

In and	Crystals	Axial growth velocity	D- L-
-----------	-----------------	------------------------------	----------

alanine doped TGS crystals, (101) faces developed more prominently than (001) faces, so the DLATGS crystals seemed to be thinner than pure TGS crystals. The (010) faces were more developed in aniline doped crystals [84]. Recently, Seif et al., [92] studied the dependence of growth rate of the faces of TGS and KDP crystals on concentration of Cr(III) [92]. They proposed the following hypothesis to explain the effect of impurities on TGS and KDP crystals. It has long been known that when a solute crystallizes from its supersaturated solution, the presence of impurities can often have a spectacular effect on the crystal growth kinetics and the habit of the crystalline phase. The impurities exhibit a marked specificity in their action as they are absorbed onto growing crystal surfaces. Absorption of impurities onto crystal faces changes the relative surface free energies of the face and may block sites essential to the incorporation of new solute molecules into the crystal lattice and hence slow down the growth. The habit is thus determined by slow growing faces. Furthermore, in TGS:Cr(III) system doping with metal ions, metal-glycine complexes are formed in solution and enter the crystal lattice in the process of growth. The structure and type of metal ion complexes formed in the TGS lattice will determine the growth rate and hence the crystal habit.

	Crystal yield g°C⁻¹per day	V₍₀₁₀₎ mm°C⁻¹per day	V₍₀₀₁₎ mm°C⁻¹ per day	V₍₀₁₀₎/V₍₀₀₁₎
TGS	0.171	0.88	0.34	2.58
TGS + Ce	0.021	0.079	0.047	1.68
TGS + Cs	0.009	0.198	0.007	28.20
TGS + L-alanine	0.192	0.89	0.44	2.02
TGS + L-alanine + Cs	0.132	0.65	0.063	10.30

Table 4 Growth data of doped TGS crystals [81]

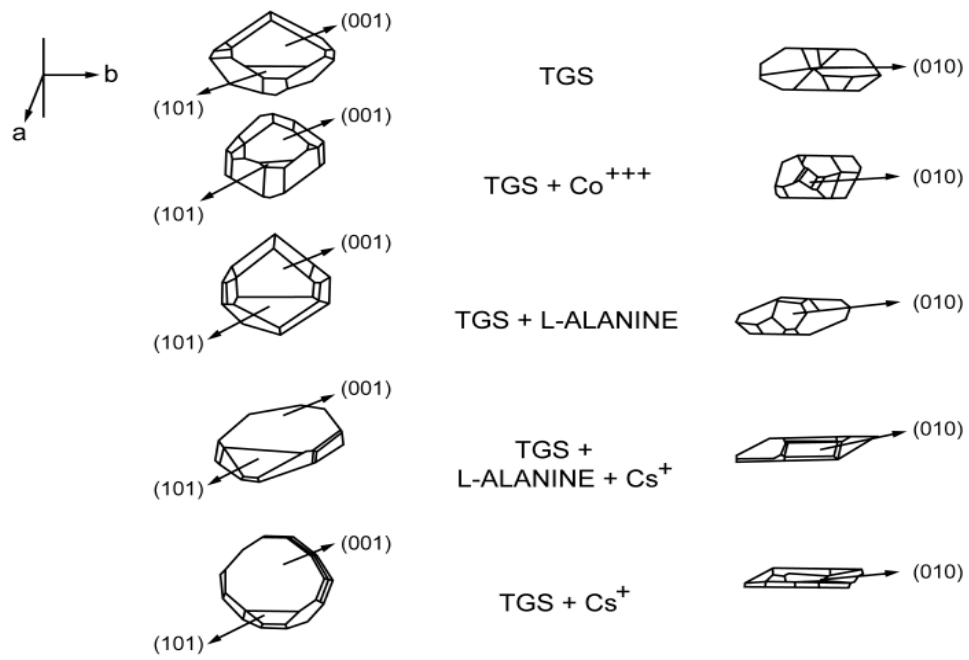


Fig. 18 Growth habit of doped TGS crystals.

It is also worthwhile to describe the effect of same impurity on different types of crystals. The growth kinetic data of TGS and KDP crystals grown in the presence of Cr(III) ions are presented in Fig. 19 and 20. This data show effect of impurity concentration on the growth rate of different faces of TGS and KDP crystals grown under constant low supersaturation. In the case of KDP crystal, the mean growth rate along [001] direction increases while along the [100] direction it remains almost constant with an increase in the concentration of Cr(III) in the solution/crystal with a slight fall below 7000 ppm. Similar type of behavior / effect of Fe(III) on growth rate of has been reported by Owczarek and Sangwal [25]. $\text{Cr}_2(\text{SO}_4)_3$ molecules are considered to dissolve as an active complex such as $[\text{Cr}(\text{H}_2\text{O})_2(\text{OH})]^{2+}$, $[\text{Cr}(\text{H}_2\text{O})_4(\text{OH})_2]^+$, $[\text{Cr}_2(\text{SO}_4)_2(\text{H}_2\text{O})_7(\text{OH})]^+$ and are assumed to adsorb on the crystal faces thereby suppressing the growth rate. The impurities adsorbed on the surface of growing crystal at low supersaturation impede movements of steps by different mechanisms depending on site of adsorption. Models of different types which describe the adsorption process and growth reduction have been reported in the literature [26-27, 36, 93]. The models assume that the impurity species (ions, molecules or atoms) are adsorbed on the crystal surface into kinks, ledges and terraces of growing surfaces. As soon as kinks and steps are occupied by impurity particles, there is a reduction in growth rates due to coverage of the crystal faces. This decrease in the growth rate can be explained on the basis of a model proposed by Sangwal et al., [32] that is based on their recent studies involving the Cu(II) - Ammonium Oxalate Monohydrate crystal system. As shown in Fig 19, the decrease in growth rate of {100} face of KDP crystals should be a kinetic effect involving a reduction in the value of the kinetic coefficient ($\beta = a \nu \exp^{(-W/kT)}$), where a is the dimension of growth units perpendicular to the step, ν is the frequency of vibration of molecules/atoms on the surface (s^{-1}), W is the activation energy for growth, k is the Boltzman constant and T is the temperature (in Kelvin)) for motion of steps on the surface. Above a certain critical concentration of impurity, there is no kinetic effect of impurity on growth kinetics. This may be due to the fact that all the active centers for crystallization are blocked, thus reducing the growth rate to zero. In our study, no growth of the {100} face was observed with more than 8000 ppm of Cr(III) impurity in the KDP solution. An increase in growth rate along the [001] direction of KDP crystals may be

caused by a decrease in the free energy of the face (thermodynamic effect); the surface energy decreases with an increase in impurity concentration as suggested by others, and hence increase in the growth rate. The above discussion suggests that the kinetic or thermodynamic effect depends on the structure of the crystal face i.e atomic arrangement also besides other factors.

Fig. 20 shows that in case of TGS crystals, the growth rate along [010] direction decreases with an increase in the concentration of Cr(III) in the growth solution. This decrease in growth rate is due to the kinetic effect as explained above for the KDP crystal system. However, there is a slight increase in the growth rate along [001] direction, with maxima around 1300 ppm of Cr(III) and then there is a decrease. According to layer growth models, the consequence of a decrease in the edge free energy is an increase in the growth rate. Additionally, a decrease in edge free energy may cause the growth mechanism to change. This effect of an initial increase followed by a subsequent decrease in growth rate with increasing concentration of impurity, has been suggested by Davey et al., [94], to opposite effects of thermodynamic and kinetic parameters. Furthermore, that ability of additives to form complexes with adventitious impurities present in a growth medium can not be ruled out, as it can alter the atomic arrangement in crystal faces. To explain the effect of impurities on growth in more detail, one needs to collect more experimental data, including studies of the micro-morphology of crystal surfaces as well as growth kinetics.

Effects of various organic dopants such as L-asparagine, L-tyrosine, L-cystine, guanidine, L-valine and other dopants on morphology, growth, mechanical and some physical properties of TGS have also been reported in the recent past [95-99]. However, no explanation is given for change in the morphology of crystals by the authors of these publications.

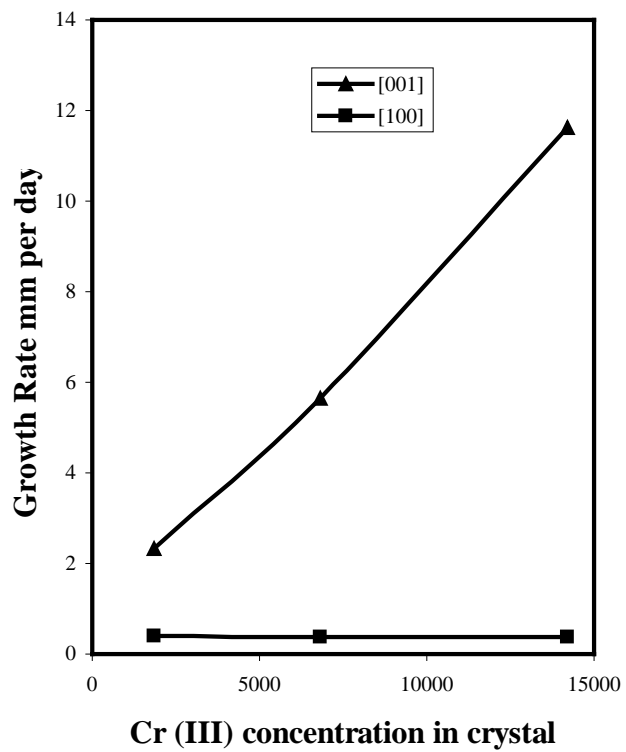


Fig. 19 Dependence of growth rate of the faces of KDP crystals on concentration of Cr(III).

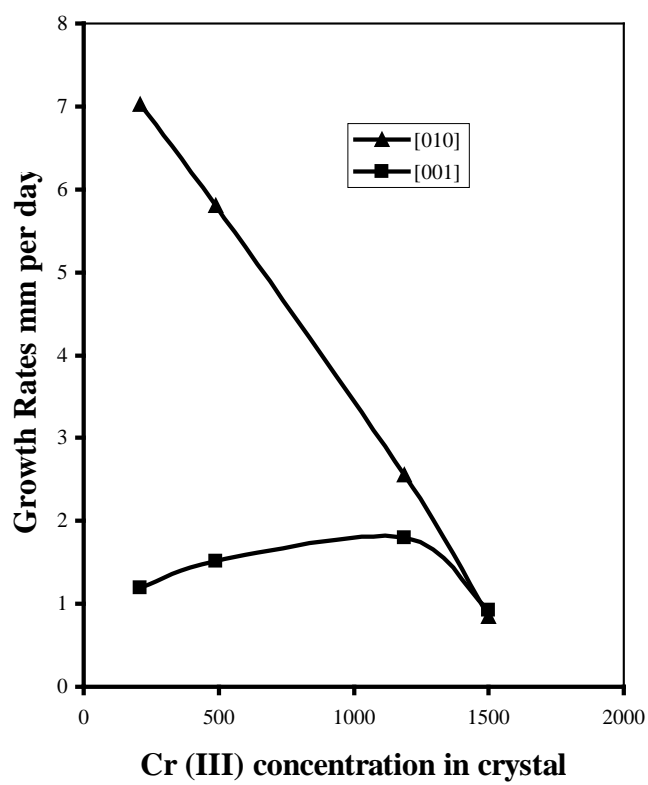


Fig. 20 Dependence of growth rate of the faces of TGS crystals on concentration of Cr(III).

7.0 SOLUTION GROWTH OF TRIGLYCINE SULFATE CRYSTALS IN MICROGRAVITY ABOARD SPACELAB-3 AND IML-1

The United States National Aeronautical Space Administration has accomplished about 115 space flight missions called STS Space Transportation Systems from STS-1 to STS-121 from 1980 to present [100].

The authors were associated with NASA's 2 missions called Spacelab-3 and International Microgravity Laboratory IML-1 for which single crystals of triglycine sulfate were grown from solution in microgravity for a period of 7 days aboard space shuttle.

The general goal of the programs within NASA's microgravity research division was to conduct basic and applied research under microgravity conditions ($10^{-6}g$) that would increase our understanding of fundamental physical, chemical, and biological processes specifically biotechnology, combustion science, fluid physics, fundamental physics, and materials science.

The microgravity environment of space provides a unique opportunity to further our understanding of various materials phenomena involving the molten, fluidic and gaseous states by reducing or eliminating buoyancy driven effects. Microgravity experiments in space are affected by residual micro-accelerations on the spacecraft deriving from atmospheric drag, reaction control systems, momentum wheels, gravity gradients, crew involvement, and other disturbances. Mostly there is no actual suggestion by the scientific community as to the microgravity level required for their experiment. The general opinion is that microgravity will reduce the influence of convection, buoyancy and sedimentation. Hardly any quantitative estimates have been made.

The anticipated results of microgravity materials science research range from establishing baselines for fundamental materials processes to generating results with more direct commercial significance. NASA's objectives for the microgravity materials science program include:

- Advancing our knowledge base for all classes of materials
- Designing and facilitating the execution of microgravity experiments that will help achieve this goal

- Determining road maps for future microgravity studies
- Contributing to NASA's Human Exploration and Development of Space enterprise
- Contributing to the national economy by developing enabling technologies valuable to the U.S. private sector

To accomplish these goals, the materials science program has tried to expand both its scientific scope and research community's involvement in microgravity research. Based on their requirements for experimental facilities most of the current materials science microgravity experiments can be divided into four general categories. The first category involves melt growth experiments, such as those used for processing multi-component alloys from the liquid. The experiments in this category frequently require high temperatures and closed containers or crucibles to prevent elemental losses. The second group includes aqueous or solution growth experiments for materials like triglycine sulfate and zeolite. These experiments usually require moderate to low temperatures. Hydrothermal processing of inorganic compounds and sol gel processing also fit in this category.

The third category of experiments involves vapor or gaseous environments, such as those used for growing mercury iodide or plasma processing. Unlike the first three categories that use containers for the parent materials and products, the fourth category involves processes and experiments that require container-less processing environments. Examples of these experiments include the formation of metallic and nonmetallic glasses during levitation melting and solidification, the float-zone growth of crystals, and the measurement of thermo-physical properties like diffusion coefficients and surface tension.

7.1 Rationale for Solution Crystal Growth in Space

In the microgravity environment of space, several physical phenomena taken for granted on earth change dramatically. Convection in solution due to density differences is greatly reduced. Crystallization and solidification are two processes that can benefit from microgravity environment. As a part of the United States National Aeronautics and Space

Administration (NASA) Microgravity and Applications Program, a study of TGS crystals growth from solution was carried out on Spacelab-3 (SL-3) and First International Microgravity Laboratory (IML-1) missions in 1985 and 1992 respectively. Crystals from solution are usually grown in a closed container of limited volume. Thus, any convection that is generated tends to lead to a circular to steady laminar convection, due to buoyancy. The density differences in the fluid can give rise from both temperature and concentration variations. On earth buoyancy driven convection may cause microscopic gas/solution inclusions and fluctuating dopants incorporation and other defects in the crystals. Besides degrading piezoelectric device performance, the growth yield of useful crystals is also severely impacted due to incorporation of these types of defects. In a low-gravity environment, convection is greatly suppressed and diffusion becomes the predominant mechanisms for thermal and mass transport. Thus, growth in microgravity can eliminate these problems and enhance our knowledge about science of crystal growth.

7.2 Solution Crystal Growth Method in Space

Since the ground solution technique could not be used in microgravity environment of space, the authors developed a new method known as cooled sting technique to grow crystals in space from solution which is described below.

7.2.1 Cooled Sting Technique

As the conventional techniques of solution crystal growth can not be used for growing crystals in space, a new technique was proposed and developed [100-102]. On earth, in the absence of stirring, conventional techniques of solution crystal growth cause a lowering of concentration of the solution in the vicinity of the growing crystal, resulting in an upward flow of solution. At constant temperature this reduction in concentration would cause growth rate to decrease rapidly. In 1-g environment, most solution growth techniques are directed towards increased convection mass transport by applying forced convection with very slow programmed cooling of saturated solution. However, in the absence of convection, a change of temperature must move inward toward the crystal by conduction. The characteristic time for this to occur is $T = L^2\rho C_p/k$, where L is the distance over which the heat must be conducted, ρ is the density, C_p is the heat capacity, and k is thermal conductivity of solution. For water, it takes 48 minutes for a temperature change of 1°C to be felt at a distance of 2 cm. This is too slow to keep a constant growth

rate. So a unique technique was developed by the authors, which uses a programmed cooling of the seed crystal itself. This is accomplished by using a cold finger (*Sting*) in direct contact with the seed crystal, which allows temperature lowering in accordance with a predetermined polynomial [103-104] for maintaining a supersaturated TGS solution near the surface of the crystal. Because of L^2 -dependence of T, it takes less time for a change of sting temperature to be transmitted through the growing crystal and to be felt at the surface. The construction of the ground based cooled sting and solution growth apparatus [103-104] are illustrated in Fig. 21 and Fig. 22, respectively. In this case, crystals are grown by lowering the sting/seed and solution temperature, thereby creating a desired supersaturation .

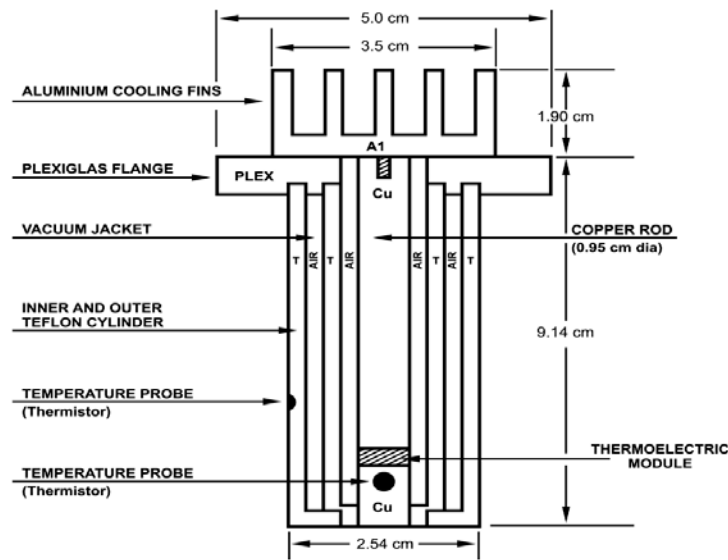


Fig. 21 Laboratory version of cooled sting assembly for crystal growth technique proposed for microgravity

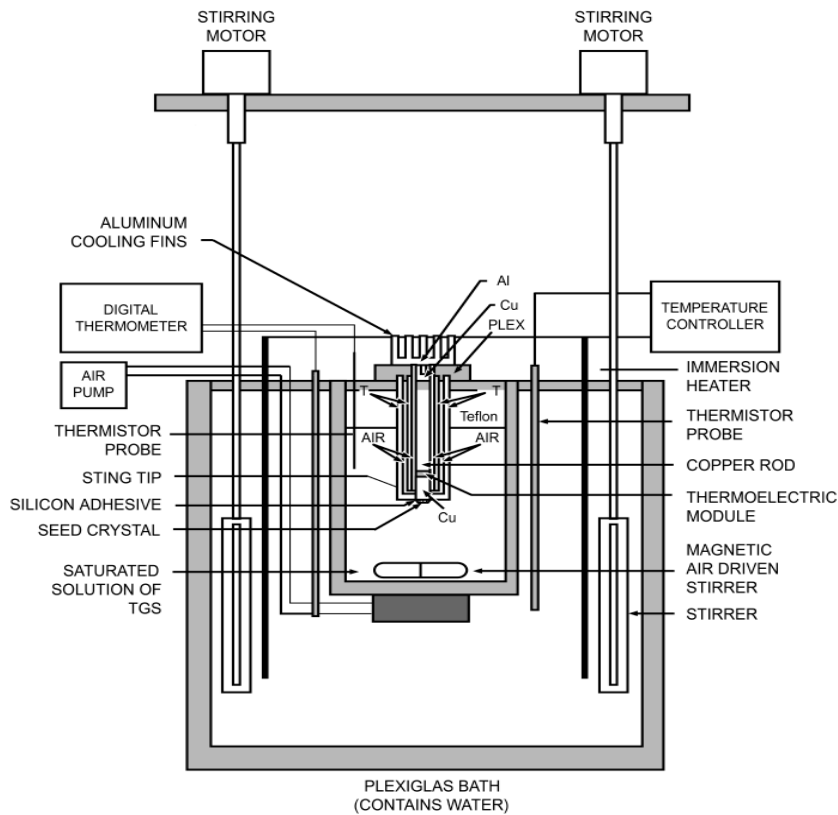


Fig. 22. Schematic diagram of the ground based cooled sting solution growth apparatus

7.2.2 Flight Hardware

The experiment in space utilizes the Fluid Experiments System (FES) and crystals are grown by a new technique developed by the authors called *Cooled Sting Technique* as described in an earlier section [101-103]. This technique utilizes heat extraction from seed crystal through a copper rod (sting), thereby creating the desired supersaturation near the growing crystal. The sting temperature profile follows a predetermined polynomial so as to get uniform growth. Fig. 23 gives a detailed diagram of the flight cell with sting incorporated in the experimental module. The FES is an apparatus with the

crystal growth cell as an integral part. It was developed by NASA and fabricated by TRW, CA

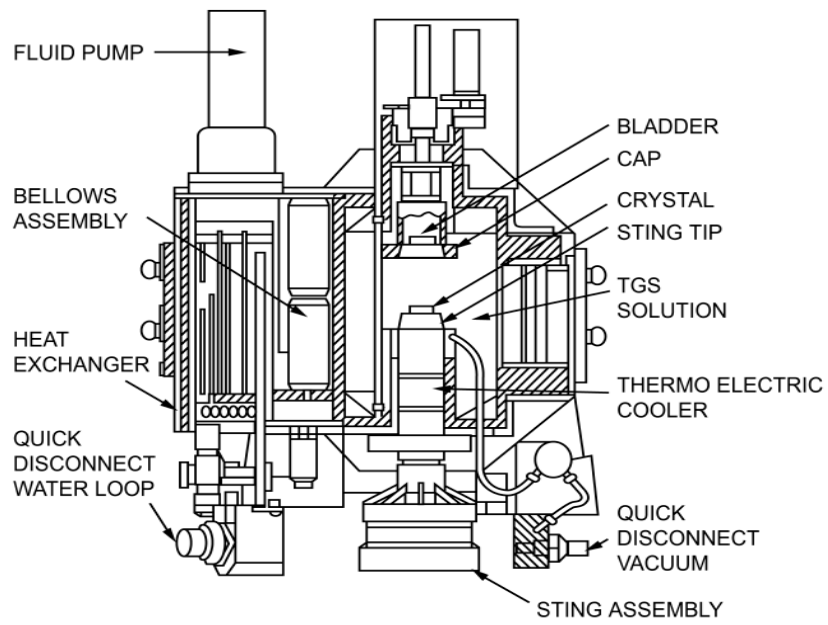


Fig. 23 Flight Crystal Growth Cell designed and developed by NASA

The cell is designed to allow a variety of holographic diagnostics and real time schlieren viewing of the crystal and the surrounding fluid. Schlieren images are transmitted down link as black and white video to reveal flow patterns and variation in fluid density. Holograms that are recorded in space give 3-D information that leads to quantitative determination of concentration fields surrounding the crystal and motion of particles if present to determine g-jitters. The modified FES incorporates holographic tomography which enables the taking of optical data through the cell at multiple angles. During SL-3 mission, two TGS crystals (named FES-2 and FES-3) were grown using (001) oriented seed-type disc (as shown in Fig. 24). The objectives of IML-1 flight experiments were:(a) to grow TGS crystals; (b) to perform holographic tomography of fluid field in the test cell in three dimensions; (c) to study the fluid motion due to g-jitter by multiple exposure holography of tracer particles (200, 400, 600 micrometers) and ; (d) to study the influence of g-jitter on crystal quality and growth rate. One of the authors (R. B. Lal) was the Principal Investigator of Spacelab-3 and IML-1 experiments. The Co-Investigators were A. K. Batra, J. Trolinger and W. R. Wilcox. During the IML-1 flight, due to serious hardware problems, only one TGS crystal was grown on a (010) oriented seed crystal. The growth surface of seed crystal was a natural (010) face (unlike experiments performed in SL-3 in which processed seeds were used.,) cut from a polyhedral TGS crystal, with a thickness of about 3.5 mm. In TGS crystal growth rate is fast (maximum) in [010] direction. On ground, good quality crystals are grown on (001) oriented seed because the growth on an (010) face is non-uniform and multifaceted. Thus, it was important to investigate the growth on an (010) oriented seed in the absence of buoyancy driven convection, where growth is expected to be mainly diffusion controlled. This crystal was grown with the undercooling of 4 °C for about 4 hours. The growth rate was estimated to be about 1.6mm/day and quality of the grown crystal was substantially good. It can be attributed to a smooth transition from dissolution to growth in space experiment.

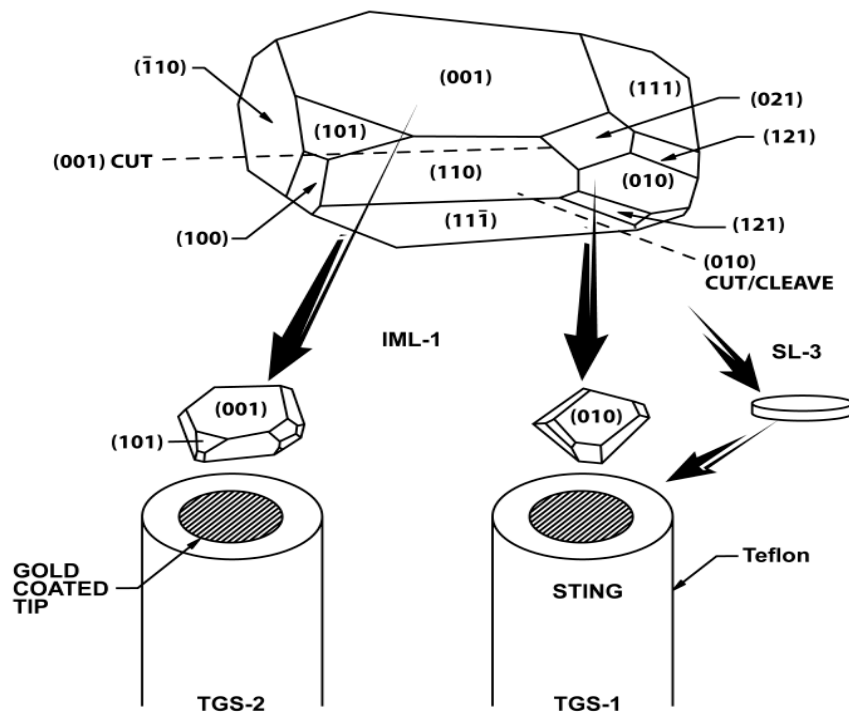


Fig. 24 TGS Seed crystals used for Growth Runs on NASA First International Microgravity Laboratory-1 (IML-1) Mission

7.2.3 Flight Optical System

The Fluids Experiment System (FES) is a fully instrumented space flight chamber that can characterize the growth process through diagnostics of the crystal environment. Fig. 25 shows the layout of optical system. Optical diagnostic instruments include two holographic cameras and a schlieren system; the output of which can be viewed in real time by TV downlink. The optical and electronic instruments provide the measure of solution concentration, temperature, convection, and growth rate and crystal properties during the time of growth.

By recording light passing through the cell as well as light scattered from the crystal, holography provided diagnostics of the fluid through holographic interferometry, and particle diagnostics through three-dimensional particle imaging velocimetry. Fig. 26 shows the layout of the optical system in which a four inch diameter, collimated He Ne (Spectra Physics 107) laser beam passes through a double window into the crystal growth chamber, through the TGS solution, across the surface of the crystal, finally emerging from a second set of windows_ The beam then continues to the hologram plane, which is approximately 20 cm away, where it is mixed with a collimated reference wave on 70 mm format roll film. The film is drawn flat on the platen by a vacuum in a unique film implementation of hologram recording for interferometry. In addition to the use of vacuum platens for recording and reconstruction, a special reconstruction process, necessary for holographic interferometry with film, described below, was developed to account for the imperfect optical quality of the film. A second holocamera views the crystal face directly from a lateral window [107]. Four types of Holograms were produced, including singly exposed and multiply exposed holograms. The back lighting of the crystal was accomplished in two different ways, each with advantages and limitations; one method employs the direct laser beam and a second employs a diffuse beam, produced by inserting a diffuser into the object beam path before the beam enters the first cell window. The diffuse beam illuminates the field with many directions and is convenient for some types of viewing. However, such illumination is not useful for interferometry or schlieren in this system. Direct illumination is also used for interferometry and schlieren. With conventional optics, the direct illumination beam would provide a single illumination and viewing angle through the field.

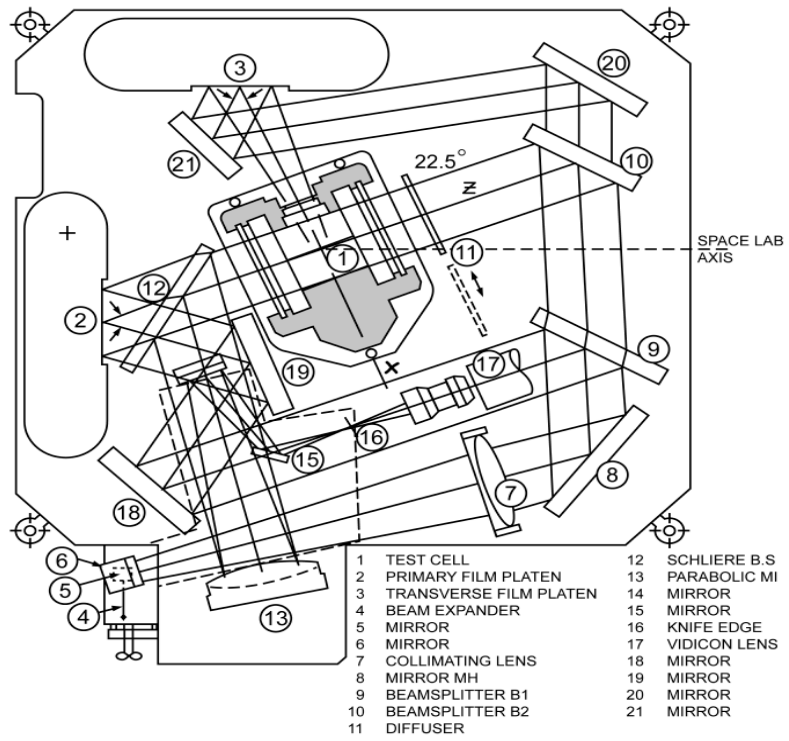
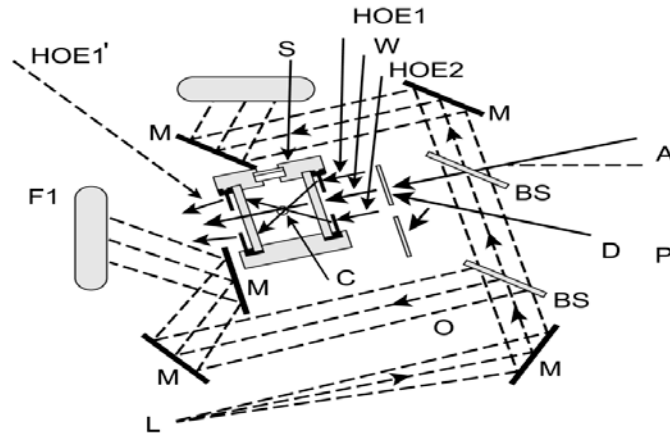


Fig. 25 Modified FES Optical System with various components



HOE 1'-Note that ray emerges at an angle to simplify separation.

A-Angle between optical axis and space shuttle axis M-mirror, BS-Beamsplitter, C-crystal, O-lens, D-removable diffusor F1-Hologram 1, F2-Hologram 2, L-HeNe laser underneath, S-side window

Fig. 26. Detailed Optical layout for the Fluid Experiment System (FES) designed and developed by TRW

Our previous experience in Spacelab 3 had taught us that more than one viewing angle is desirable. We achieved multiple viewing angles in IML-1 through the use of windows equipped with holographic optical elements (HOEs). The input window contains HOEs that convert the single input beam into three beams that pass over the crystal at angles of 0° and $\pm 23.5^\circ$. The opposite window contains HOEs that redirect these beams to the recording film plane so that they can all be recorded and again separated during reconstruction. Consequently, each recording comprises three superimposed, but independently viewable holograms. The schlieren system is viewed by T⁺; allowing real time viewing both by the crew and by the TV downlink. A

primary use of the schlieren system is to view and judge the transition of the crystal from a dissolution phase to a growth phase since control of this transition is considered to be critical in producing a high quality crystal. The knife edge in the schlieren system was set so that when the crystal was dissolving, light rays entering the resulting higher refractive index region above the crystal would be refracted in the direction of the crystal be removed by the knife edge, and appear dark in the image. When the transition from dissolving to growing was made, the region immediately above the crystal would be depleted of solute, thus reducing the refractive index and causing the refracted rays to pass above the knife edge, causing a bright region to appear above the crystal within the larger, dark region of higher concentration. The method proved to be an extremely sensitive way to identify the transition from dissolving to growth.

7.3 Results and Discussion

The flight TGS crystals were examined with a high-resolution monochromatic synchrotron X-radiation diffraction technique, both before and after slicing for the fabrication of infrared detectors to check the lattice regularity, identify inclusions and dislocations, draw inferences about growth mode and stability, and locate the interface between the seed and the new growth. The experiments were performed at the National Synchrotron Light Source at Brookhaven National Laboratory in collaboration with Dr. Bruce Steiner of the United States National Institute of Standards and Technology (NIST). The performance of materials is determined by their structure; in this performance, irregularity typically plays a leading role. The growth of crystals in low-g has long been of interest because of anticipation that reduction in gravitational forces would strongly affect crystal growth and therefore the nature of resulting irregularities. Many factors affect crystal growth, and because these can interact strongly with one another, the understanding of the structural variation necessary for its effective exploitation has not been fully achieved. A knowledge of irregularities in space and earth grown crystals, developed in conjunction with an understanding their genesis and detailed affects on properties, would be an important challenge. Such knowledge is expected also to contribute to dramatically improve single crystal production, both in space and on the earth. The local acceptance angle for diffraction from the uncut flight TGS-1 crystal, 1-2 arc seconds (Fig. 27), indicates extraordinary crystal quality [108]. Polystyrene particles

that had been included in the space-grown material in IML-1 experiment are observed as small imperfections in Fig. 27(b). Also, clearly distinguishable in Fig. 27 (b) is the faceted growth mode. Two sets of edge dislocations in the seed, one [101]-oriented and the other [001]-oriented, were noted as well in images taken in Laue geometry; but they appear not to have affected the space growth. Observation of the cut edge of the crystal, Fig. 27(d), shows continuity between the seed at the top. The demarcation between the seed and the space-grown material is indistinct. High-resolution imaging of terrestrial crystals has shown that the surface treatment of the seed crystal is critical to growth perfection. The ground control TGS crystals were of extremely high perfection. Slice next to many possible flight seeds were examined by high-resolution diffraction imaging. The selection of the flight seed was based on the perfection of the slice next to the seed crystal.

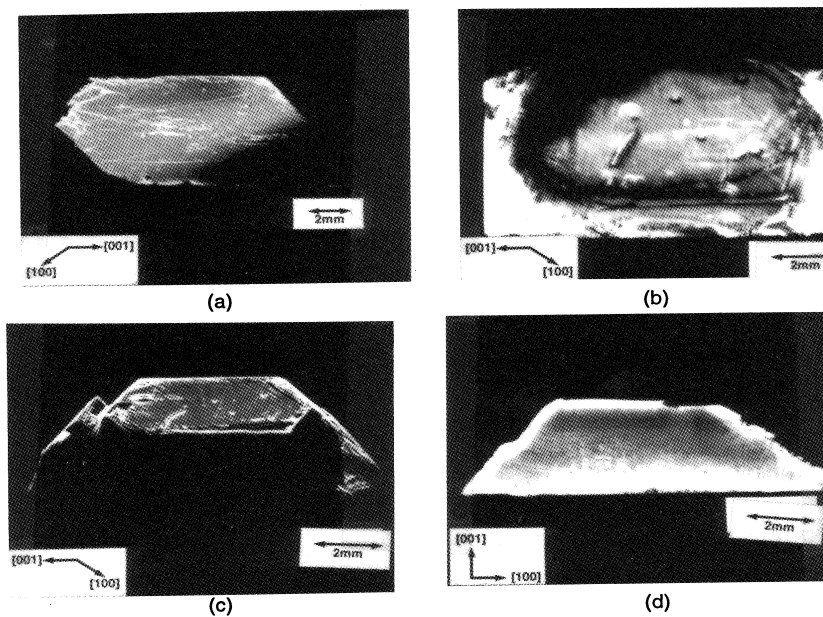


Fig. 27. High Resolution Synchrotron X-Ray Radiation Diffraction Imaging of 1-g and μg Grown TGS Crystals

Infrared detectors from the flight and ground control crystals were fabricated at EDO/Barnes Engineering Division, Shelton, CT. The detectivity (D^*) and other parameters for these infrared detectors are shown in Fig. 28. The detector characteristics are given in Table 5. The detectivity (D^*) for I.R. detectors fabricated from the IML-1 crystal shows an improvement over the ground grown crystals and crystals grown on Spacelab 3.

The particles motion of three different size particles were mapped using the techniques described elsewhere [106, 107]. The combined effects of fluid convection, particle interaction, residual gravity, shuttle maneuvers, and g-jitters have been observed. However, the interferograms show several noteworthy features. When the crystal enters a growth phase, the solution in the region near the crystal is depleted of solute, thus reducing its refractive index below the surrounding fluid, creating a hemispherical cap of fringes over the crystal as show in Fig.29. The stability of this cloud in the interferograms confirmed that the crystal was growing in a diffusion controlled process. The cloud did show, however, that the process was not completely axisymmetric, a condition by equipment problems that were encountered during the mission.

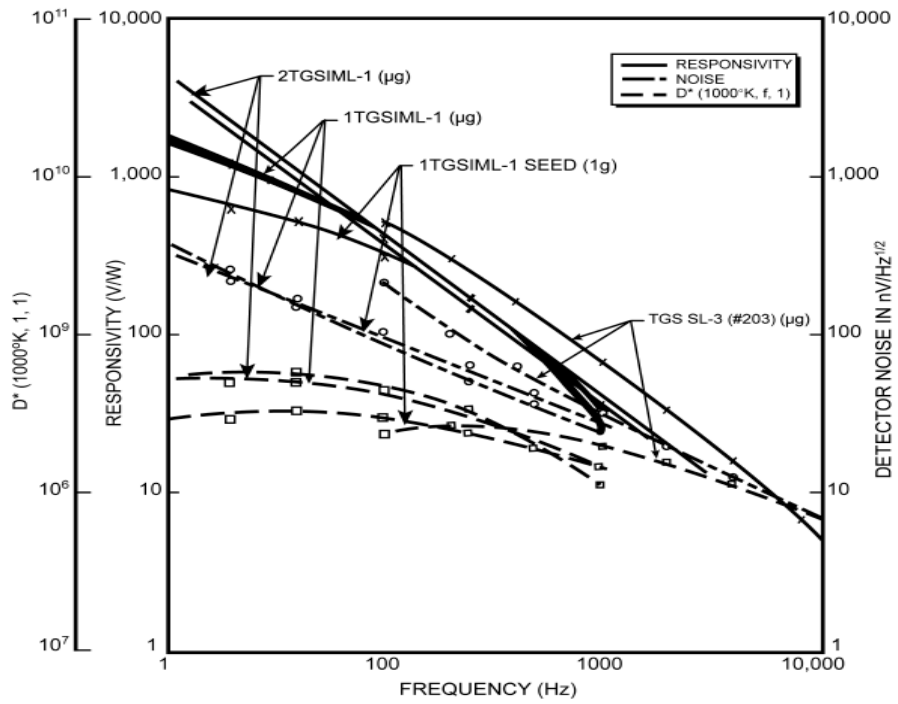
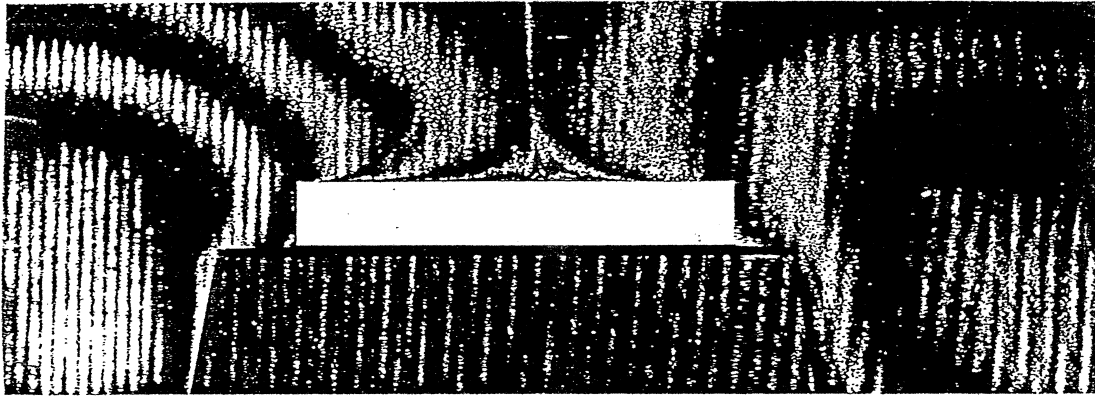


Fig. 28. Relevant parameters of infrared detectors fabricated from 1-g and micro-g grown TGS crystals

Table 5 Detector characteristics of space grown TGS crystals

Crystal (TGS)	Noise nV/Hz^{1/2}	Responsivity (V/W)	Detectivity (1000° K,f,1) X 10⁸	f Hz	Remarks
SL-3/FES2-TGS (μg-grown)	320	510	0.99	100	Area = 0.3 X 3 mm, Blackened
IML-1TGS Seed (1g-grown)	418	320	2	100	Area = 1 X 1 mm, no window
IML-1TGS (μg-grown)	90	400	4.2	100	Area = 1 X 1 mm
IML-1TGS (1g-grown)	98	420	4.5	100	Area = 1 X 1 mm
IML-1TGS (μg-grown)	100	340	3	100	Area = 1 X 1 mm



Earth



Spacelab 3

Fig. 29. Interferograms of Concentration Field in TGS Solution on Earth and in microgravity onboard Spacelab-3

To sum up, in spite of problems with the operation of the FES, two important objectives were attained in the IML-1 experiment: (a) A high quality TGS crystal was grown; (b) The particle dynamics experiment was successful.

In spite of a limited time and fast growth, the growth on the (010) face was substantially uniform over a period of 18h. The growth on the (010) face on ground is mostly non-uniform. The local acceptance angle for diffraction from the uncut crystal, 1-2 arcs second, indicates extraordinary crystal regularity. Polystyrene particles of three sizes that had been occluded by the growing TGS were observed as small imperfections

in the grown crystal. The observations of the cut edge of the flight crystal (TGS-1) show continuity between the seed at the bottom and the space growth at the top, indicating a high degree of epitaxy of the space grown material. The demarcation between the seed and the space grown material is indistinct, indicating a smooth transition from dissolution to growth so that solvent inclusions are not formed between the seed and the grown layer. Experiments on earth have shown that such inclusions tend to result in dislocations that propagate through subsequently grown material and degrade properties. The infrared detectors fabricated from the TGS-1 flight crystal show improved detectivity (D^*) compared to ground samples and even with detectors fabricated from crystals grown on Spacelab-3. The dielectric loss in the IML-1 crystal is lower than in ground crystals and in crystals grown in Spacelab-3.

8.0 Protein Crystal Growth

The human body contains thousands of different proteins, which play essential roles in maintaining life. A protein's structure determines the specific role that proteins play in the human body; however, researchers lack detailed knowledge about the structures of many proteins. The crystallization of proteins has three major applications: (1) structural biology and drug design, (2) bio-separations, and (3) controlled drug delivery. In the first application, the protein crystals are used with the techniques of crystallography to ascertain the three-dimensional structure of the molecule. This structure is indispensable for correctly determining the often complex biological functions of these macromolecules. The design of drugs is related to this, and involves designing a molecule that can exactly fit into a binding site of a macromolecule and block its function of the disease pathway. Producing better quality crystals will result in more accurate 3D protein structure, which in turn means its biological function can be known more precisely, also resulting in improved drug design. The second application: bio-separations refer to the downstream processing of the products of fermentation. Typically, the desired product of the fermentation process is a protein (e.g. insulin) , which then needs to be separated from biomass. Crystallization is one the commonly employed techniques for separation of protein. It has the advantage of being a benign separation process, that is, it does not cause the protein to unfold and lose its activity. The other application of protein: controlled drug delivery is also very important. Most drugs are

cleared by the body rapidly following administration, making it difficult to achieve a constant desired level over a period of time. When the drug is a protein such as insulin or Alfa-interferon, administering the drug in the crystalline form shows promise of achieving such controlled delivery. The challenge is to produce crystals of relatively uniform size so that dosage can be prescribed correctly.

8.1 Protein Crystal Growth Methods

Protein crystallization is inherently difficult because of the fragile nature of protein crystals. Proteins have irregularly shaped surfaces, which result in the formation of large channels within any protein crystal. Therefore, the no-covalent bonds that hold together the lattice must often be formed through several layers of solvent molecules. In addition, to overcoming the inherent fragility of protein crystals, the successful production of x-ray worthy crystals is dependent upon a number of environmental factors because so much variation exists among proteins, with each individual requiring unique conditions for successful crystallization. Therefore, attempting to crystallize a protein without a proven protocol can very tedious. Some factors that require consideration are protein purity, pH, concentration of protein, temperature, and the precipitants. In order to initiate crystallization the protein solution has to be brought to a thermodynamically unstable state of supersaturation. The solution can be brought back to the stable equilibrium state through precipitation of the protein, which is the most frequent process, or through crystallization. The supersaturation state can be achieved by several techniques: evaporation of solvent molecules, change of ionic strength, change of pH, change of temperature or change of some other parameter.

Two of the most commonly used methods for protein crystallization fall under the category of vapor diffusion [109-2-110]:

- (i) Hanging drop method
- (ii) Sitting drop method

Both the above cited methods entail a droplet containing purified protein, buffer and precipitants in higher concentration. Initially, the droplet of protein solution contains an insufficient concentration of precipitant for crystallization, but as water vaporizes from the drop and transfer to the reservoir, the precipitant concentration increases to a level optimal for crystallization. Since the system is in equilibrium, these optimum conditions

are maintained until the crystallization is complete. Figures 30 and 31 depict the hanging drop and sitting drop systems, respectively. The hanging drop method differs from the sitting drop method in the vertical orientation of the protein solution drop within the system. It is important to mention that both methods require a closed system that is, the system must be sealed off from outside using an airtight container. It is worthy of mentioning that reservoir solution usually contains buffer and precipitant. Protein solution contains the same compounds, but in lower concentrations. The protein solution may also contain trace metals or ions necessary for precipitation. For instance, insulin is known to require trace amounts of zinc for crystallization.

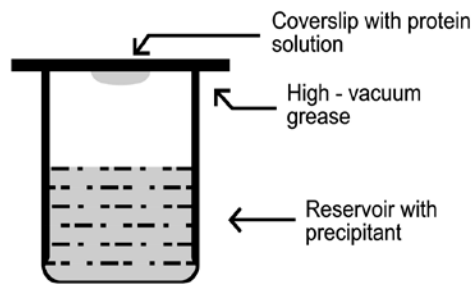


Fig. 30 Schematic diagram of hanging drop method

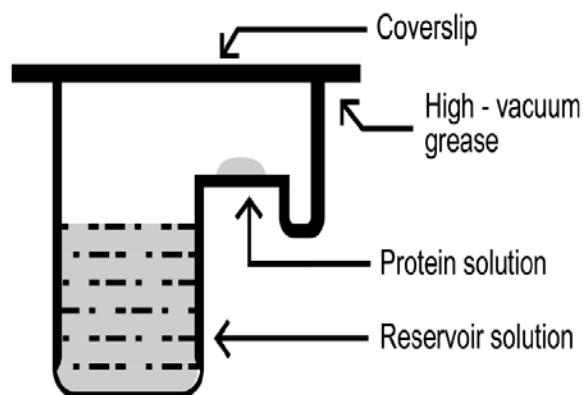


Fig. 31 Schematic diagram of sitting drop method

8.2 Protein Crystal Growth Mechanisms

From the presence of well defined facets on most protein crystals one can unambiguously conclude that growth occurs via the spreading of layers from growth step sources such as dislocations and 2D nuclei. This has been confirmed on a molecular level. Ex-situ electron microscopy observations have resolved individual growth steps on (010) and (110) faces of tetragonal lysozyme [111] that, contrary to recent claims [112, 113], are of monomolecular height. In-situ atomic force microscopy of lysozyme has produced particularly instructive images of growth step generation at screw dislocations outcrops and of 2D nucleation-induced islands.

Most recent atomic force microscopy observations on a larger number of other proteins and viruses [114] have reproduced the whole body of growth morphology and kinetics scenarios known for inorganic solution growth. These include layer spreading from dislocations and 2D nuclei, interaction between growth steps from sources of different activities, and impediment of step propagation by foreign particles. Particle engulfment was observed to often result in dislocation formation. Crystallites that

impinged on the interface became either epitaxially aligned with main crystal, or remained misaligned and caused various defects during further growth. There appears to be even some indication of kinetic roughening on certain facets of some proteins [115].

8.3 Protein Crystal Growth in Microgravity

The microgravity environment aboard space craft in low Earth orbit provides a convection and sedimentation free environment for the study and applications of fluid-based systems. With the advent of the United States' Space Shuttle, scientists had regular access to such environments and many experiments were initiated, including those in protein crystallization. After many trials it became clear that for several proteins, crystallization in microgravity environment resulted in bigger and better crystals. In some instances, crystals that could not be crystallized on the ground at all were found to crystallize in space. Conversely, for numerous proteins the space environment was found to be no better or was worse than ground-based conditions. As a result of these observations, NASA has become one of the leading federal agencies in prompting and funding protein crystallization research. Efforts are directed at both utilizing the space environment to improve the crystallization of novel proteins and in fundamental studies of the causes (if any) of the improvement in protein crystals produced in microgravity. The results from flying more, and studying in more detail, have "significantly altered" attitudes towards space-based protein crystal growth. "Persuasive explanations" have emerged, and a strong theoretical model has emerged to explain why space-based growth is better.

Since the inception of protein crystal growth in microgravity research by Littke [118], several research groups have developed microgravity hardware and experiments [118-123]. Some of those are listed below:

- (i) Hand-held protein crystallization apparatus for microgravity (HH-PCAM) [124]
- (ii) Diffusion-controlled crystallization apparatus for microgravity (DCAM) [125]
- (iii) High-density protein crystal growth system (HDPCG) [126]
- (iv) Protein crystal growth facility (PCF) [127]

- (v) A multi-user facility-based protein crystallization apparatus for microgravity (PCAM) [124]
- (vi) Advanced protein crystallization facility (APCF) [125]

Several thousand individual protein crystal growth experiments have been flown using the PCAM facility hardware aboard the US Space Shuttle. According to developer of this facility hardware represents a pioneering development in design and deployment of space flight hardware which are based on disposable interface elements [124]. Furthermore, it has resulted in an ultra high resolution structure and first example of neutron diffraction achieved as a result of protein crystal growth in microgravity [127]. Additionally, using this facility, fundamental differences in protein partitioning in microgravity have been documented which represent the first direct experimental observation of the factors contributing to quality improvements in the growth of protein crystals in microgravity [128]. The other important hardware referred to as diffusion-controlled crystallization apparatus for microgravity (DCAM) which utilizes the dialysis method and allows the equilibration rate of each individual experiment to be passively controlled from several days to several months. It is worth mentioning that precision control rate of supersaturation has routinely produced macro crystals of size 5 mm to 1.25 cm for a variety of protein in this hardware. Analysis of serum albumin, ferritin, lysozyme, bacteriorhodopsin, and nucleosome core particles exhibit superior diffraction properties as compared to ground-based controls [125]. Further improvements of the hardware is going on for International Space Station where scientists can learn more about the mechanisms of the growth, and X-ray analysis can be done aboard the Space Station [126].

9.0. CONCLUDING REMARKS

Bulk high quality single crystals are required for use in fabricating devices for various technological applications. Since crystal growth is a complicated process that depends on many parameters that can interact and the complete process is not well understood. This is one of the reasons to grow crystals in microgravity of space to separate omnipresent convection on Earth and have only diffusion controlled growth. Authors have attempted to give an comprehensive overview of the various problems encountered in the solution growth of single crystals on Earth and in space experiment

based on their experience for almost 3 decades. The solutions of the various problems encountered during growth on ground and in spaceflight experiments are described. This chapter shall serve as a foundation for those who desire to initiate a research program in the growth of bulk single crystals of technological importance that can be grown from low temperature solution technique. A brief review of the crystal growth fundamentals is presented including key techniques for solution crystal growth such as solubility determination, design of various crystal growth systems including mechanical and electronic crystal motor reciprocating arrangement. Three generations of modifications to solution crystallizers designed and fabricated in the laboratory and the crystallizer for space growth cooled sting technique advanced by the authors are described. A number of solution grown crystals grown at Alabama A&M University are shown. A detailed description of the crystal growth experiments on an important infrared material triglycine sulphate and difficulties encountered in the space crystal growth experiment aboard space shuttle in NASA Spacelab-3 and the first International Microgravity Laboratory (IML-1) missions is given. Since basic principles of solution growth technique are shared by protein crystal growth, basic techniques of protein crystal growth are briefly mentioned and the efforts of protein crystal growth in microgravity are also discussed.

ACKNOWLEDGEMENTS

The authors are grateful for helpful discussions with a number of graduate students and other physics faculty in the department of physics at Alabama A&M University. Authors are thankful to Mr. Garland Sharp for his expert machining work and Mr Jerry Johnson for his glass blowing jobs in the design of various crystal growth systems described in this work. This work was partially supported under NSF-HBCU RISE program HRD-0531183 and U.S. Army Space and Missile Defense Command, Contract W9113M-04-C-0005. Two of the authors (MDA and RBL) would like to acknowledge support from NASA Administrator's Fellowship Program (NAFP) through United Negro College Fund Special Programs (UNCFSP) Corporation under their Contract No. NNG06GC58A.

References

1. H. A. Meirs and F. Isaac: The spontaneous crystallization, Proc. Roy. Soc. London **A79**, 322-325 (1987).
2. K. Sangwal: Growth kinetics and surface morphology of crystals grown from solutions: Recent observations and their interpretations, Prog. Cryst. growth and Charact. Mat. **36**(3), 163-248 (1998).
3. I. F. Nicolau: Growth kinetics of potassium-dihydrogen phosphate crystals in solution, Kristall and Technik **9**(11), 1255-1263 (1974).
4. R. Janssen-Van Rosmalen and P. Bennema, J. Garside: The influence of volume diffusion on crystal growth, J. Cryst. Growth **29**, 342-352 (1975).
5. A. Chianese: Growth and dissolution of sodium perborate in aqueous solutions by using RDC technique, J. Cryst. Growth **91**, 39-49 (1988).
6. K. Sangwal: On the mechanism of crystal growth from solutions, J. Cryst. Growth **192**, 200-214 (1998).
7. Y. Wang, X. L. Yu, D. I. Sun, S. T. Yin: Mass transport and growth kinetics related to the interface supersaturation of lithium formate monohydrate, Cryst. Res. Technol. **36** (4-5), 441-448 (2001).
8. N. Zaitseva, L. Carman: Rapid growth of KDP-type crystals, Prog. Cryst. growth and Charact. Mat. **43**, 1-118 (2001).
9. I. V. Melikhov, L. B. Berliner: Crystallization of salts from supersaturated solutions ; diffusion kinetics, J. Cryst. Growth **46**, 79-84 (1979).
10. P. Bennema: Spiral growth and surface roughening: development since Burton, Cabrera and Frank, J. Cryst. Growth **69**, 182-197 (1984).
11. X. Y. Liu, K. Malwa, K. Tsukamoto: Heterogeneous two dimension nucleation and growth kinetics, J. Chem. Phys. **106**(5), 1870-1879 (1997).
12. Alexander F. Izmailov, Allan S. Myerson: Momentum and mass transfer in supersaturation solutions crystal growth from solution, J. Cryst. Growth **174**, 263-368 (1997).
13. Mirosława Rak, Karel Izdebski, Andrzej Brozi: Kinetic Monte Carlo study of crystal growth from solution, Computer Phys. Comm., **138**, 250-263 (2001).

14. F. Rosenberger, B. Mutaftschiev (ed.): *Interfacial Aspects of Phase Transformation* (D. Reidel Publishing Company 1982).
15. A. A. Chernov: Present day understanding of crystal growth from aqueous solutions, *Prog. Cryst. growth and Charact.* **26**, 121-151 (1993).
16. Rajeev Mohan, Allan S. Myerson: Growth kinetics: a thermodynamic approach, *Chem. Engn. Sci.* **57** , 4277-4285 (2002).
17. C. M. Pina, A. Putnis, J. M. Astilleros: The growth mechanisms of solid solutions crystallization from aqueous solutions, *Chemical Geology* **204**, 145-161 (2004).
18. I. Sunagawa, K. Tsukamoto, K. Maiwa, K. Onuma: Growth and perfection of crystals from aqueous solution: Case studies on Barium nitrate and K-Alum, *Prog. Cryst. and Charact.* **30**, 153-190 (1995).
19. William R. Wilcox: Influence of convection on the growth of crystals from solution, *J. Cryst. Growth* **65**, 133-142 (1983).
20. Ivan V Markov: *Crystal Growth for Beginners* (World Scientific, NJ, USA 2004)
21. Ichiro Sunagawa: *Crystals Growth, Morphology and Perfection* (Cambridge University Press, Cambridge, UK 2005).
22. Tomoya Ogawa: A phenomenological Analysis of crystal growth from solutions as an irreversible process, *Jap. J. Appl. Phys.* **16**(5), 689-695 (1977).
23. S. Veintemillas-Verdaguer: Chemical aspects of the effect of impurities in crystal growth, *Prog. Cryst. Growth and Charact.* **32**, 76-109 (1996).
24. K. Sangwal: Kinetics effects of impurities on the growth of single crystals from solutions, *J. Cryst. Growth* **203**, 197-212 (1999).
25. I. Owczarek, K. Sangwal: Effect of impurities on the growth of KDP crystals: Mechanism of adsorption on (101) faces, *J. Cryst. Growth* **102**, 574-580 (1990).
26. K. Sangwal: Effects of impurities on the crystal growth processes, *Prog. Cryst. and Charact.* **32**, 3-43 (1996).
27. E. Kirkova, M. Djarova, B. Donkova: Inclusions of isomorphism impurities during crystallization from solutions, *Prog. Cryst. Growth and Charact.* **32**, 111-134 (1996).

28. M. Rauls, K. Bartosch, M. Kind, St. Kuch, R. Lacmann, A. Mersmann: The influence of impurities on crystallization kinetics-a case study on ammonium sulfate, *J. Cryst. Growth* **312**, 116-128 (2000).
29. E. Mielniczek-Brzoska, K. Gielzak-Kocwin, K. Sangwal: Effects of Cu(II) ions on the growth of ammonium oxalate monohydrate crystals from aqueous solutions: growth kinetics, segregation coefficient and characterization of incorporation sites, *J. Cryst. Growth* **212** , 532-542 (2000).
30. K. Sangwal, E. Mielniczek-Brzoska, J. Bore: Effect of Mn(II) ions on the growth of ammonium oxalate monohydrate crystals from aqueous solutions: Growth habit and surface morphology, *Cryst. Res. Technol.* **38(2)**, 103-112 (2003).
31. Noriaki Kubota, Masaaki Yokota, J. W. Mullin : Supersaturation dependence of crystal growth in solutions in the presence of impurity, *J. Cryst. Growth* **182** , 86-94 (1997).
32. K. Sangwal, E. Mielniczek-Brzoska : On the effect of Cu(II) impurities on the growth kinetics of ammonium oxalate monohydrate crystals from aqueous solutions, *Cryst. Res. Technol.* **36** (8-10), 837-849 (2001).
33. K. Sangwal, E. Mielniczek-Brzoska, J. Bore: Study of segregation coefficient of cationic impurities in ammonium oxalate monohydrate crystals during growth from aqueous solutions, *J. Cryst. Growth* **244**, 183-193 (2002).
34. K. Sangwal, T. Palcznska: On the supersaturation and impurity concentration dependence of segregation coefficient in crystals grown from solutions, *J. Cryst. Growth* **212**, 522-531 (2002).
35. Sv. P. Delineshev: Growth of crystals in the presence of impurities, a hypotheses based on a kinetic approach, *Cryst. Res. Technol.* **33** (6) 891-897 (1998).
36. K. Sangwal: Kinetic effects of impurities on the growth of single crystals from solutions, *J. Cryst. Growth* **203**, 197-212 (1999).
37. A. S. Myerson and S. M. Jang: A comparison of binding energy and metastable zone width for adipic acid with various additives. *J. Cryst. Growth* **156**, 459-466 (1995).

38. D. Aquilano, M. Rubbo, G. Mantovani, G. Sgualdino and G. Vaccari: Equilibrium and growth forms of sucrose crystals in the {h0l} zone, *J. Cryst. Growth* **74**, 10-20 (1986).
39. D. Aquilano, M. Rubbo, G. Mantovani, G. Sgualdino and G. Vaccari: Equilibrium and growth forms of sucrose crystals in the {h0l}zone, *J. Cryst. Growth* **83**, 77-83 (1987).
40. A. A. Chernov and V. V. Sipyagin: Peculiarities in crystal growth aqueous solutions connected with their structure, in *Current Topics in Materials Science*, E. Kaldis, Ed., Vol 5 pp279-333, North-Holland, Amsterdam, 1980.
41. Crystal growth of technologically important electronic materials, K. Byrappa, H. Klapper, T. Ohachi, R. Fornari Eds. Allied Publishers PVT. Limited, New Delhi, 2003.
42. M. D. Aggarwal, T. Gebre, A. K. Batra, M. E. Edwards, R. B. Lal, B. G. Penn, D. O. Frazier:Growth of nonlinear optical materials at Alabama A&M University, *Proc. of SPIE*, vol.4813: Crystal Materials for Nonlinear Optical Devices and Microgravity Science,52-65 (2002).
43. M. D. Aggarwal, W. S. Wang, K. Bhat, P. G. Penn and D. O. Frazier: Photonic Crystals: Crystal growth processing and physical properties, in *Handbook of Advanced Electronic and Photonic Materials and Devices*, H. S. Nalwa. Ed. Academic Press, New York, vol.9 pp193-228 (2001)
44. Heinz K. Henisch: *Crystal Growth in Gels* (Dover Publications, Inc. New York 1970).
45. A. F. Barton, *Handbook of solubility parameters and other cohesion parameters*, CRC Press, Boca Raton, FL 1983.
46. J. Novotny: A crystallizer for the investigation of conditions of growth of single crystals from solutions, *Kristall and Technik* **6(3)**, 343-352 (1971)
47. M.D. Aggarwal, J. Choi, W. S. Wang, K. Bhat, R. B.Lal, R.B., A.D Shields, B. G. Penn, D. O. Frazier: Solution growth of a novel nonlinear optical material: L-histidine tetrafluoroborate, *J. Cryst. growth* **204**, 179-182 (1999).
48. W. S. Wang, M. D. Aggarwal, J.Choi. K.Bhat, T. Gebre, A.D Shields, B. G. Penn, D. O. Frazier: Solvent effects and polymorphic transformation of organic nonlinear optical crystal L-pyroglutamic acid in solution growth processes, *I.*

- Solvent effects and growth morphology, *J. Cryst. growth* **198/199**, 578-582 (1999).
49. C. Owens, K. Bhat, W. S. Wang, A. Tan, M.D. Aggarwal, P.G. Penn, D.O. Frazier: Bulk growth of high quality nonlinear optical crystals of L-arginine tetrafluoroborate (L-AFB), *J. Cryst. Growth* **225**, 465-469 (2001).
 50. R. B. Lal, H. W. Zhang, W. S. Wang, M. D. Aggarwal, Howard W. H. Lee, B. G. Penn: Crystal growth and optical properties of 4-aminobenzophenone crystals for NLO applications, *J. Cryst. growth* **174**, 393-397 (1997).
 51. H. W. Zhang, A. K. Batra, R. B. Lal: Growth of large methyl-(2,4-dinitrophenyl)-aminopropanoate: 2-methyl-4-nitroaniline crystals for nonlinear applications, *J. Cryst. Growth* **137**, 141-144 (1994).
 52. Michelle Renee Simmons: MS thesis "An investigation of crystals matrices of single crystals doped with rare earth ions" Alabama A&M University, Normal, AL. (USA) 2002.
 53. Jiann-Min Chang, Ashok K. Batra and Ravindra B. Lal: Growth and characterization of doped TGS crystals for infrared devices, *Cryst. Growth & Design* **2(5)**, 431-435 (2002)
 54. R. B. Lal and M. D. Aggarwal: Reciprocating Crystallizer: Automatic crystallizer grows crystals from aqueous solutions, *NASA Tech. Briefs* **8**, 419 (1984)
 55. M. D. Aggarwal and R. B. Lal: Simple low-cost reciprocating crystallizer for solution crystal growth, *Rev. Sci. Instr.* **54**, 772-773 (1983)
 56. A. K. Batra and S. C. Mathur, Reciprocating arrangement for solution crystal growth, *Res. Indust.* **20**, 29 (1984).
 57. A. K. Batra, C. R. Carmichael-Owens, M. Simmons, M. D. Aggarwal and R. B. Lal: Design of a solution crystal growth crystallizer with versatile electronic reciprocal motion control for a crystal holder, *Cryst. Res. Technol.* **40(8)**, 757-760 (2005).
 58. Ashok K. Batra, Mohan D. Aggarwal and Ravindra B. Lal: Growth and characterization of doped DTGS crystals for infrared sensing devices, *Mat. Lett.* **57**, 39-43 (2003).

59. Franco Jona and S. Shirane: *Ferroelectric Crystals* (Dover Publications Inc., New York, USA 1993)
60. R. B. Lal and A. K. Batra: Growth and properties of triglycine (TGS) sulfate crystals: Review, *Ferroelectrics* **142**, 51-82 (1993)
61. E. A. D. White, J. D. C. Wood and V. M. Wood: The growth of large area, uniformly doped TGS crystals, *J. Cryst. Growth* **32**, 149-156 (1976).
62. B. Brezina, M. Havrankova, M. VASA: Enhanced growth of non-polar{001} growth sectors of deuterated triglycine sulfate doped with L-alanine (LADTGS), *Cryst. Res. Technol.* **27(1)**, 13-20 (1992).
63. S. Satapathy, S. K. Sharma, A. K. Karnal, V. K. Wadhawan, Effects of seed orientation on the growth of TGS crystals with large (010) facets needed for detector applications, *J. Cryst. Growth* **240** 196-202 (2002).
64. Mohsen Banan, Growth of pure and doped triglycine sulfate crystals for pyroelectric infrared detector applications, MS thesis, 1986 Alabama A&M University, Normal, AL 35762, USA.
65. Deng Zhao-De: A new method of growth of ferroelectric crystal, *Ferroelectrics* **39**, 1237 (1981).
66. F. Moravec and J. Novotny, Study on the growth of triglycine sulphate single crystals, *Kristall und Technik* **7**, 891-902 (1972).
67. W. K. Burton, N. Cabrera and F. C. Frank, *Philos. Trans. R. Soc., London*, **243**, 299 (1951).
68. L. N. Rashkovich, *Sov. Phys. Crystallog*, **28**, 454 (1983).
69. J. Novotny, F. Moravec and Z. Solc: The role of surface and volume diffusion in the growth of TGS single crystals, *Czech. J. Phys.*, **B23**, 261-266 (1973).
70. J. Novotny and F. Moravec: Growth of TGS from slightly supersaturated solutions, *J. Cryst. Growth* **11**, 329-335 (1971).
71. D. A. Reiss, R. L. Kroes and E. E. Anderson: Growth Kinetics of the (001) face of TGS below the ferroelectric transition temperature, *J. Cryst. Growth* **84**, 7-10 (1987).

72. F. Moravec and J. Novotny: A contribution to the study of the influence of impurities on the growth and some physical properties of TGS single crystals, *Kristall and Technik* **6(3)**, 335-342 (1971).
73. R. V. Whipps, R. S. Cosier and K. L. Bye: Orthorhombic diglycine sulphate, *J. Mat. Sci.*, **7(12)**, 1476-1477 (1972).
74. E. Dominquez, R. Jimenez, J. Mendiola and E. J. Vivas: Diglycine sulphate- an interesting new dielectric crystal species, *J. Mat. Sci.*, **7(3)**, 363-364 (1972).
75. M. S. Tsedrik, V. N. Ulasen and G. A. Zaborovski: *Kristall and Technik*, **10(1)**, 49 (1975).
76. E. J. Weidmann, E. A. D. White and V. M. Wood: Induced growth anisotropy in TGS crystals, *J. Mat. Sci. Lett.* **7**, 719-720 (1972).
77. L. Szczepanska: Growth investigations of single crystal sulphates containing molecular glycine groups, *Kristall and Technik*, **11**, 265-271 (1976).
78. L. Prokopova, J. Novotny, Z. Micka, V. Malina, Growth of triglycine sulphate crystals doped by cadmium phosphate, *Cryst. Res. Technol.*, **36**, 1189-1195 (2001)
79. G. R. Pandya and D. D. Vyas: On growth and morphological studies of TGS single crystals, *Cryst. Res. and Technol.*, **16**, 1353-1358 (1981).
80. R.B. Lal, S. Etminan and A.K. Batra: Effect of simultaneous organic and inorganic dopants on the characteristics of triglycine sulfate crystals, *Proc. 9th IEEE Intern. Symp on applications of Ferroelectrics*, p.695-697 (1994)
81. M. Banan, A. K. Batra and R. B. Lal: Growth and morphology of triglycine sulphate (TGS) crystals, *J. Mat. Sci. Lett.* **8**, 1348-1349 (1989).
82. M. Banan, R. B. Lal, A. K. Batra and M. D. Aggarwal: Effect of poling on the morphology and growth rate of TGS crystals, *Cryst. Res. Technol.* **24(3)**, K53 (1989).
83. N. Nakatani, Ferroelectric domain structure and internal bias field in DL- α -Alanine-doped triglycine sulfate, *Jpn. J. Appl. Phys.* **30** (12A), 3445-3449 (1991).
84. J. Eisner, the physical properties of TGS single crystals, grown from aqueous TGS solutions containing Aniline *Phys. Status Solidi* **43**, K1-K4 (1977).

85. F. Moravec, J. Novotny, and J. Strajblova, Single crystals of triglycine sulphate containing palladium Czech. J. Phys., **23**, 855-862 (1977).
86. A. S. Sidorkin and A. M. Kostsov, Exoelectron emission from a ferroelectric crystal of triglycine sulfate with defects, Soviet Physics-Solid State **33(8)**, 1383-1384 (1991).
87. L. Yang, A. K. Batra and R. B. Lal: Growth and characterization of TGS crystals grown by cooled sting technique, Ferroelectrics **118(1-4)**, 85 (1991).
88. N. Nakatani: Ferroelectric domain structure and Internal Bias Field in DL- α -Alanine doped triglycine sulfate, Jap. J. Appl. Phys., **30**, 3445-3449 (1991)
89. B. Brezina and M. Havrankova: Orientation of structure and crystals of TGS and TGS doped with D, al or L, al, Cryst. Res. Technol, **20**, 781-786 (1985).
90. G. M. Loiacono and J. P. Dougherty: Final Technical Report (contract no DAAK70-77-C-0098) submitted to Night Vision and Electro-optics Laboratories, Fort Belvoir, Virginia, 1978
91. O. W. Wang, C. S. Fang: Investigation of the solution status of TGS and ATGSP crystals, Cryst. Res. Technol. **27**, 245-251 (1992).
92. Selemeni Seif, Kamala Bhat, Ashok K. Batra, Mohan D. Aggarwal, Ravindra B.Lal: Effect of Cr(III) impurity on the growth kinetics of potassium dihydrogen phosphate and triglycine sulfate grown from aqueous solutions, Mat. Lett. **58**, 991-994 (2004).
93. V. A. Kuznetov, T. M. Okhrimenko, M. Rak: Growth promoting effect of organic impurities on growth kinetics of KAP and KDP crystals, J. Cryst. Growth **193**, 164-173 (1998).
94. R. J. Davey in: E. J. de Jong, S. J. Jancic (Eds), *Industrial Crystallization*, vol 78 p 169 (North-Holland, Amsterdam 1979)
95. K. Meera, R. Muralindharan, A. K. Tripathi, P. Ramasamy: Growth and characterization of l-threonine, dl-threonine, l-methionine admixed TGS crystals, J. Crystal Growth **263**, 524-531 (2004).
96. Genbo Su, Youping He, Hongzhi Yao, Zikong Shi, Qingjin: A new pyroelectric crystal L-lysine-doped THS (LLTGS), J. Cryst. Growth **209**, 220-222 (2000).

97. G . Arunmozhi, E. De Matos Gomes, J. Ribeiro : Dielectric properties of L-Asparagine doped TGS (Asp-TGS) crystals, *Ferroelectrics* **295**, 87-95 (2003).
98. J. Novotny, J. Zelinkam F. Moravec: Broadband infrared detectors on the basis of PATGS/Pt(IV) single crystals, *Sensors and Actuators A* **119**, 300-304 (2005).
99. S. Kalainathan, M. Beatrice Margaret, T. Trusan: Morphological changes of L-asparagine doped TGS crystal, *Cryst. Engn.* **5**, 71-78 (2002)
100. http://www.nasa.gov/mission_pages/shuttle/shuttlemissions/list_main.html
101. R. B. Lal, R. L. Kroes: Solution growth of crystal on Spacelab-3, Proceedings of the 24th AIAA Science Meeting, Reno, Nevada, Jan 6-8, 1985.
102. R. B. Lal, M. D. Aggarwal, R. L. Kroes, W. R. Wilcox: A new technique of solution crystal growth, *Phys. Status Solidi (A)* **80**, 547- 551 (1983).
103. A. K. Batra, R. B. Lal, M. D. Aggarwal : Electrical properties of TGS crystals grown by new technique, *J. Mat. Sci. Lett.* **4**, 1425-1427 (1985).
104. R. B. Lal, M. D. Aggarwal, A. K. Batra, R. L. Kroes: Solution growth of crystals in zero-gravity, Final Technical Report, NASA contract number **NAS8-32945** (1987).
105. L. Yang, A. K. Batra, R. B. Lal: Growth and characteristics of TGS crystals grown by cooled sting technique, *Ferroelectrics* **118(1-4)**, 85-89 (1991).
106. R. B. Lal, A. K. Batra, J. D. Trolinger and W. R. Wilcox: TGS crystal growth experiment on the first international microgravity laboratory (IML-1). *Microgravity Quarterly* **4(3)**, 186-198 (1994).
107. R. B. Lal: Solution growth of crystals in low-gravity, Final Technical Report, NASA Contract number **NAS8-36634** (1995).
108. B. Steiner, R. Dobbyn, D. Black, H. Burdette, M. Kuriyama, R. Spal, L. van den Berg, A. Fripp, R. Simchick, R. Lal, A. Batra, D. Mathiesen, B. Ditchek: High resolution diffracting imaging of crystals grown in microgravity and closely related terrestrial crystals, NIST Technical Note **1287** (1991).
109. Duncan E. McRee: *Practical Protein Crystallography*, San Diego: Academic Press, 1993 (pp1-23).
110. Gale Rhodes: *Crystallography Made Crystal Clear*, pp8-10, pp29-38 (Academic Press, San Diego 1993)

111. S. D. Durbin and G. Feher: Studies of crystal growth mechanisms of proteins by electron microscopy, *J. Mol. Biol.* **212**, 763-774 (1990).
112. E. Forsythe and M. L. Pusey: The effects of temperature and NaCl concentration on tetragonal lysozyme face growth rates, *J. Cryst. Growth* **139**, 89-94 (1994).
113. A. Nadaraja, E. L. Forsythe and M. L. Pusey: The averaged face growth rates of lysozyme crystals: the effect of temperature, *J. Cryst. Growth* **151**, 163-172 (1995)
114. W. Littke, C. John: Protein single crystal growth under microgravity, *Science*, **225**, 203-204 (1984)
115. F. Rosenberger: Protein crystallization, *J. Cryst. Growth* **166**, 40-54 (1996)
116. S. Gorti, E.L. Forsythe and M.L. Pusey: Measurable characteristics of lysozyme crystal growth, *Acta Cryst. D* **61**, 837-843 (2005).
117. <http://science.nasa.gov/ssl/msad/pcg/>
118. W. Littke and C. John: Protein single crystal growth under microgravity, *J. Cryst. Growth*, **76**, 663-672 (1986)
119. L. J. DeLucas, F.L Suddath, R. S. Snyder, R. Naumann, M. B. Broom, M. Pusey, V. Yost, B. Herren, D. Carter, B. Nelson, E. J. Meehan, A. McPherson, C. E. Bugg: Preliminary investigations of protein crystal growth using the space shuttle, *J. Cryst. Growth* **76**, 681-693 (1986)
120. L. J. DeLucas, C. D. Smith, H. W. Smith, V. K. Senadhi, S.E. Senadhi, S. E. Ealick, D. C. Carter, R. S. Snyder, P. C. Weber, F. R. Salemme, D.H. Ohlendorf, H.M. Einspahr, L. L. Clancy, M. A. Navia, B. M. McKeever, T. L. Nagabhushan, G. Nelson, A. McPherson, S. Koszelak, G. Taylor, D. Stammers, K. Powell, G. Darby, C. E. Bugg: Protein crystal growth in microgravity, *Science*, **246**, 651-653 (1989)
121. S.Simic-Stefani, M.Kawaji, H.U. Hu: G-jitter induced motion of a protein crystal under microgravity, *J. Cryst. Growth*, **294**,373-384 (2006).
122. A. McPherson: Virus and protein crystal growth on earth and in microgravity, *J. Phys. D*, **26**, B104-B112 (1993).
123. D. C. Carter, T. E. Dowling: Protein crystal growth apparatus for microgravity, US Patent No. 5,643,540 (1997)

124. Daniel C. Carter, Brenda Wright, Teresa Miller, Jenny Chapman, Pam Twigg, Kim Keeling, Kerry Moody, Melissa White, James Click, John R. Ruble, Joseph X. Ho, Lawana Adcock-Downey, Tim Dowling, Chong-Hawn Chang, Paul Ala, John Rose, B. C. Wang, Jean-Paul Declercq, Chrisitine Evrard, John Rosenberg, Jean-Pierre Wery, Davis Clawson, Mark Wardell, W. Stallings, A. Stevens: PCAM: a multi-user facility-based protein crystallization apparatus for microgravity, *J. Cryst. Growth* **196**, 610-622 (1999)
125. Daniel C. Carter , Brenda Wright, Teresa Miller, Jenny Chapman, Pam Twigg, Kim Keeling, Kerry Moody, Melissa White, James Click, John R. Ruble, Joseph X. Ho, Lawana Adcock-Downey, Gerard Bunick, Joel Harp : Diffusion-controlled crystallization apparatus for microgravity (DCAM): flight and ground-based applications, *J. Cryst. Growth* **196**, 602-609 (1999)
126. Lawrence J. DeLucas, K.M. Moore, M.M. Long, R. Rouleau, T. Bray, W. Crysel, L. Weise : Protein crystal growth in space, past and future, *J. Cryst. Growth* **237-239**, 1646-1650 (2002)
127. J. P. Declereq, C. Evrard, D. C. Carter, B. S. Wright, G. Etienne, J. Parello: A crystal of a typical EF-hand protein grown under microgravity diffracts x-rays beyond 0.9 Å resolution, *J. Cryst. Growth* **196**, 595-601 (1999).
128. D. C. Carter, K. Lim, J. X. Ho, B. S. Wright, P. D. Twigg, T. Y. Miller, J. Chapman , K. Keeling, J. Ruble, P. G. Vekilov, B. R. Thomas, F. Rosenberger, A. A. Chernov: Lower dimer impurity incorporation may result in higher perfection of HEWL crystals grown in microgravity: A Case Study, *J. Cryst. Growth* **196**, 623-637 (1999).